Colossal-magnetoresistive manganite thin films

2001 J. Phys.: Condens. Matter 13 R915

(http://iopscience.iop.org/0953-8984/13/48/201)

INSTITUTE OF PHYSICS PUBLISHING JOURNAL OF PHYSICS: CONDENSED MATTER

J. Phys.: Condens. Matter **13** (2001) R915–R944 PII: S0953-8984(01)22519-3

TOPICAL REVIEW

Colossal-magnetoresistive manganite thin films

W Prellier, Ph Lecoeur and B Mercey

Laboratoire CRISMAT, CNRS UMR 6508, Boulevard du Maréchal Juin, 14050 Caen Cédex, France

E-mail: prellier@ismra.fr

Received 25 May 2001, in final form 29 August 2001
Published 16 November 2001
Online at stacks.iop.org/JPhysCM/13/R915

Abstract

Mixed-valence perovskite manganites ($Re_{1-x}A_xMnO_3$ where Re = rare earth, A = alkaline earth) provide a unique opportunity to study the relationships between the structure and the magnetotransport properties due to an interplay among charge carriers, magnetic coupling, orbital ordering and structural distortion. This makes these compounds very exciting from both the basic research and from the technological viewpoint. As the technology pursued with these materials requires film growth, extensive studies have been made on materials synthesis, structural and physical characterization and device fabrication. In this article, the results from the different experimental techniques and the effects of the deposition procedure of the manganite thin films are first reviewed. Second, the relation between the structural and the physical properties is mentioned, and the influence of strains discussed. Finally, possible applications of manganite thin films in spin electronics are presented.

1. Introduction

The last decade has seen the emergence of epitaxial metal oxide films as one of the most attractive subjects for the condensed matter community. The emergence of such interest was primarily stimulated by the discovery of high-temperature superconductors (HTSC) and more recently by the discovery of the colossal-magnetoresistance (CMR) effect in thin films of manganese oxides $Re_{1-x}A_xMnO_3$ (where Re is a rare earth and A is an alkaline earth) [1–5]. CMR materials exhibit large changes in electrical resistance when an external magnetic field is applied [6, 7].

The doped manganites are mixed valence, with Mn^{3+} ($3d^4$) and Mn^{4+} ($3d^3$). For the octahedral site symmetry of MnO_6 the configurations become $t_{2g}^3e_g^1$ for Mn^{3+} and t_{2g}^3 for Mn^{4+}. In the double-exchange mechanism, the e_g electrons are considered as mobile charge carriers in interactions with localized Mn^{4+} ($S = 3/2$) spins. The carrier hopping avoids strong on-site Hund's rule exchange energy J_{ex} when the spins are aligned ferromagnetically. (Note that if the Mn spins are not parallel or if the Mn–O–Mn bond is bent, the electron transfer becomes

more difficult and mobility decreases.) J_{ex} is much larger that the e_g bandwidth and, thus, the conduction electrons are highly spin polarized in the ground state. Making use of this idea, correlations of the half-ferromagnetic character of the CMR materials were found [8]. Theoretical and experimental studies indicate that the small-polaron effects including Jahn–Teller distortion also play important roles for the transition and transport measurements [9].

These oxide materials are important from a fundamental point of view since they offer a chemical flexibility that enables new structures and new properties to be generated and, consequently, the relations between the structure, electronic, magnetic and transport properties to be studied.

Since most technological applications require thin films on substrates, the ability to prepare such films and understand their properties is of prime importance. The synthesis of the first high-temperature superconducting oxide thin films almost 15 years ago generated great interest in the thin-film community. This resulted in the development of various techniques, guided by the importance of preparing high-quality thin films of superconductor compounds, including sputtering, molecular beam epitaxy (MBE) and metal–organic chemical vapour deposition (MOCVD), but the most popular technique is probably pulsed laser deposition (PLD) [10]. This latter method is used extensively to synthesize cuprates and HTSCs, which are now routinely made in laboratories, and it has been easily and rapidly adapted for manganites. Another reason for this quick transfer of technology is that these oxide materials crystallize in a perovskite structure like the HTSCs and, in some sense, they are quite similar [11, 12]. Moreover, the manganite oxides are highly sensitive to the strain effect, and this offers the possibility of studying its influence upon various properties such as insulator-to-metal transition temperature (T_{IM}), Curie temperature (T_C), structure and microstructure/morphology. The renewed interest in the manganite materials has resulted in a large volume of published research in this field.

In the present article, we present a brief review of the experimental work done in the past seven years. The deposition procedure and its influence (through deposition temperature, oxygen pressure, post-annealing, substrate type, ...) upon the magnetotransport properties will be discussed. In the particular case of thin films, work was mainly devoted to substrate-induced strain and thickness dependence, and we will describe the experimental situation. Finally, since much of the interest to the community of the CMR thin films lies in their use in devices, some applications of these materials will also be presented. Due to the extremely large amount of research data published in this field, there will unfortunately inevitably be some missing citations, and we apologize to the authors of these in advance.

2. Deposition procedures, structure and properties

CMR manganite materials are compounds crystallizing in a perovskite-like structure, which, in addition to manganese and oxygen, contain rare earths and/or lanthanide cations. The prototype compound is $La_{1-x}Ca_xMnO_3$, but there are many other related structures. Numerous studies have been performed on hole-doped $La_{0.7}A_{0.3}MnO_3$ manganites (where A = Sr or Ca) since these CMR materials exhibit the highest Curie temperatures seen so far (often associated with an insulator-to-metal temperature transition). Such high-temperature transitions, close to room temperature, make them suitable for applications [13]. As previously stated, there are many different compounds due to the fact that the A-site cation can be a lanthanide or a rare earth. Thus, a number of systems have been studied in the form of thin films including: La–Ca–Mn–O [1–3, 5, 14–24], La–Sr–Mn–O [25–32], La–Ba–MnO [33–35], La–Pb–Mn–O [36–40], La–Mn–O [41–43], Nd–Sr–Mn–O [44–52], Sm–Sr–Mn–O [53, 54], Pr–Ca–Mn–O [55–59], Pr–Sr–Mn–O [60–64], La–Sn–Mn–O [65], La–K–Mn–O [66], La–Ce–Mn–O [67] and Bi–Sr–Mn–O [68]. To detail the situation in terms of synthesis, this section is divided into three parts.

First, in section 2.1, we will review the parameters that govern the growth of these oxides (temperature, oxygen pressure etc), and we will consider the progress made in the synthesis of these materials. We will also focus on the different techniques that were used for the growth of thin films. Then in section 2.2, we will discuss the different studies that were carried out with the aim of achieving an understanding of the structure and the microstructure of the thin films for the simple perovskite oxides and also of the results for the double-ordered perovskites. Finally, some physical measurements will be presented (section 2.3).

2.1. Synthesis of manganite films

2.1.1. Simple perovskite: $AMnO_3$. The manganite thin films were been mainly prepared using the pulsed laser deposition technique [2, 29, 44, 69–71]. The principle of this technique is relatively simple. A pulsed laser beam ablates a dense ceramic target of the desired material. In the presence of a background gas (usually oxygen), a plasma is produced and condenses on the heated substrate. Typical lasers used for manganite are excimer UV with KrF at $\lambda = 248$ nm [56, 72], XeCl at $\lambda = 308$ nm [24, 55, 71] or ArF at $\lambda = 193$ nm [35]. A frequency-tripled Nd-YAG at $\lambda = 355$ nm [16,41] or quadrupled Nd-YAG at $\lambda = 266$ nm [38] may also be used. A cross-beam deposition scheme utilizing two Nd-YAG lasers was also used to grow $Pr_{0.65}Ca_{0.35}MnO_3$ thin films on $LaAlO_3$ [58]. However, the utilization of high oxygen pressure during the PLD growth prevents the use of a reflection high-energy electron diffraction (RHEED) system in order to control *in situ* the different stages of the growth. By using a more oxidizing gas (atomic oxygen, ozone, ...) and a differential pumping system, the electron path in the high-pressure oxygen atmosphere can be reduced, and thus the specular beam of the RHEED can be monitored in order to observe the oscillations (see figure 1 for a typical experimental set-up). High-quality manganite thin films were fabricated in this way [27,34,73]. Persistent intensity of the RHEED is observed and the roughness of the films is low, around one unit cell [27].

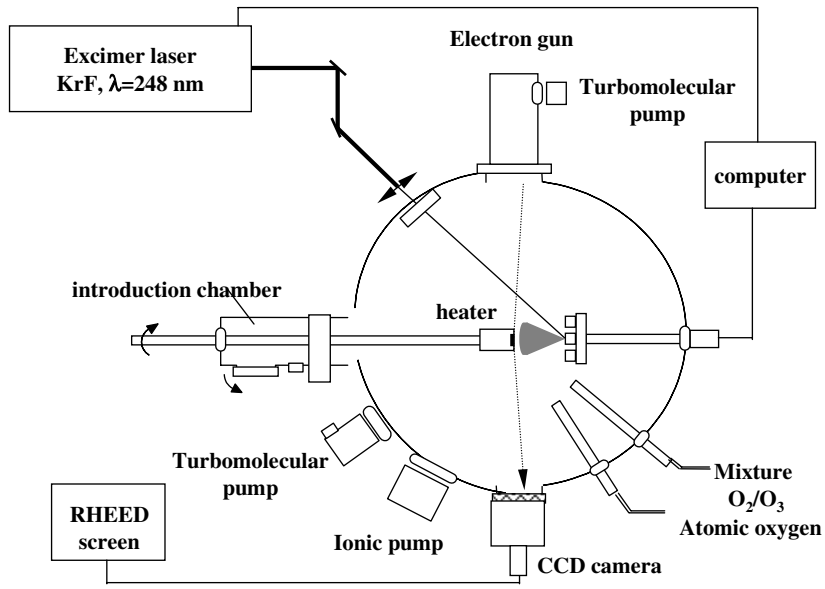

Figure 1. The typical experimental set-up for a pulsed laser deposition system used for growing oxides.

A second popular deposition technique is magnetron sputtering, which can be RF [32,37,60,74,75] or DC [23,30,61,76,77]. Reactive sputtering is particularly useful for large-area films, but the deposition of complex oxides, comprising several cations, is difficult because of a possible change in the material composition between the target and the film. Nonetheless, in these two techniques (PLD and sputtering) highly dense ceramic targets are utilized, and the configuration is usually 'on-axis'. This means that the plane of the substrate is perpendicular to the particle flux. Samples can also be produced by sputtering [52, 78, 79] and PLD [3, 18] in the 'off-axis' configuration. In the case of PLD, this decreases the surface roughness and avoids the formation of droplets associated with laser deposition. Ion beam sputtering [80], electron beam/thermal coevaporation [66] and molecular beam epitaxy [81–83] have also been utilized to make manganite thin films. MOCVD was used to prepare high-quality thin films of various compositions [26, 84–86]. Briefly, metal–organic precursors are dissolved in an ether and injected into the low-pressure apparatus. In contrast to the methods previously described, this one does not require a high vacuum but allows deposition at higher oxygen pressure. Others methods used for making manganite thin films are nebulized spray pyrolysis [51, 87] and the sol–gel technique [88].

Various gases, such as O_2 [56, 89], N_2O [44, 45], ozone [90] and a mixture of argon and oxygen atmospheres [60, 79, 91], result in oxygen-stoichiometric films. The background gas pressure is important for the oxidation process. Thus, the emission of the gas-phase oxide of Mn during pulsed laser deposition of manganites in O_2 and N_2O atmospheres was studied. The studies show that both oxidation in the gas phase and at the surface are required in order to obtain optimized properties. It was found that N_2O increases the oxidation of Mn in the plasma plume, leading to an improvement of the magnetic properties of $La_{0.67}Sr_{0.33}MnO_3$ [92].

The deposition conditions (oxygen pressure P_{O_2}, deposition temperature T_S, laser fluence, ...) can drastically influence the properties [16, 22, 64, 93, 94]. For $Nd_{0.7}Sr_{0.3}MnO_3$ grown on (100)-oriented $LaAlO_3$ [45], the maximum resistivity peak shifts to lower temperatures as the deposition temperature decreases (the optimum T_C of 175 K is obtained for $T_S = 615\ ^\circ$C). Yamada *et al* [38] have shown that T_{IM} decreases with either T_S or P_{O_2} in $La_{1-x}Pb_xMnO_3$. The deposition temperature also strongly influences the microstructure of $Pr_{0.7}Sr_{0.3}MnO_3$, since films grown at low temperature exhibit a columnar growth with well-connected grains while those deposited at higher temperature are poorly connected with platelet-like crystals [64].

In addition, it has also been shown that *in situ* [16, 95] or *ex situ* [22, 31, 32, 96, 97] oxygen annealings are necessary to obtain the optimized properties. In particular, the post-annealing of the films can lead to significant modification of the oxygen content and optimizes the physical properties [29, 98, 99] such as T_{IM} [46], T_C and the CMR effect [1, 3, 5]. This annealing effect is necessary to achieve the optimum oxygen concentration of the films. Depending on the nature of the film and on the growth conditions, annealing is used either to fully oxidize the film (oxidative annealing) or to remove extra oxygen (reductive annealing). The effect of annealing was also observed in films annealed in N_2 atmosphere (see figure 2 for $La_{1-x}Sr_xMnO_3$) [98]. The T_{IM}-transition shifts upon annealing to higher temperature and the MR ratio increases slightly. The magnetic transition also occurs at higher temperature after annealing. For example, the Curie temperature, T_C, is found to increase from 200 K for as-deposited $La_{0.8}MnO_3$ film to 320 K after the fourth thermal treatment (see figure 3) [99]. In fact, the changes under annealing can also be seen in the position of the diffraction peak [56, 99]: the out-of-plane parameter decreases, which relates to an increase of the Mn^{3+}/Mn^{4+} ratio [20, 99]. This annealing effect can lead to an improvement in physical properties (like in $La_{0.8}Ca_{0.2}MnO_3$ where the T_{IM}-value is higher than that of the bulk; reference [100]) but sometimes the resistivity peak is lower by more than 100 K [101].

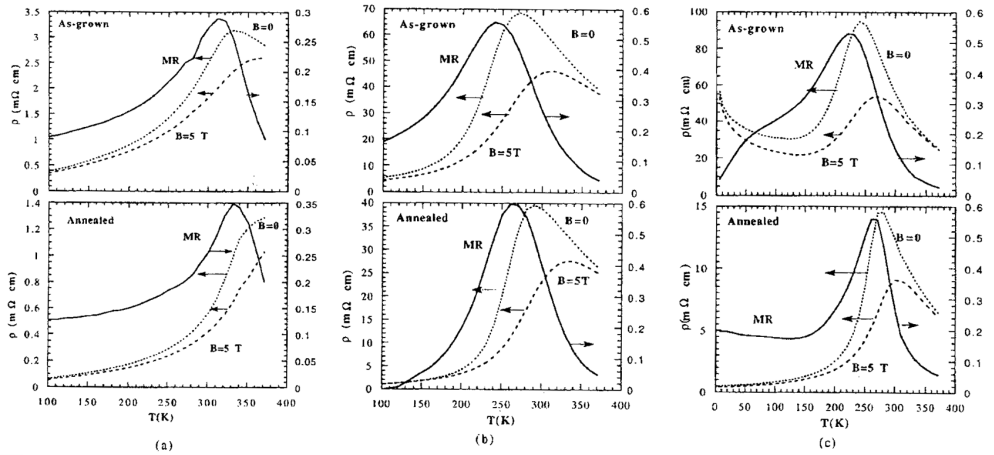

Figure 2. $\rho(T)$ and the MR ratio of $La_{1-x}Sr_xMnO_3$ thin films in zero field and a field of 5 T, for as-grown films (top) and films annealed at 950 °C for 10 h in pure N_2 gas (bottom). (a) $x = 0.33$, (b) $x = 0.2$ and (c) $x = 0.16$. (Reproduced from reference [98].)

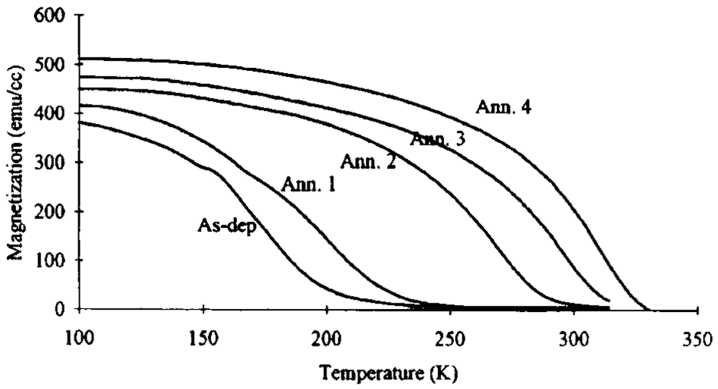

Figure 3. $M(T)$ for as-deposited and post-annealed $La_{0.8}MnO_{3-\delta}$ films. Annealing 1: 600 °C, 3 h; annealing 2: 600 °C, 24 h; annealing 3: 700 °C, 3 h; annealing 4: 800 °C, 3 h. (Reproduced from reference [99].)

In fact, Prellier *et al* have shown that the entire phase diagram is different in the ferromagnetic region of $La_{1-x}Ca_xMnO_3$ ($0 < x < 0.5$) [20] as compared to the bulk (in terms of transport and magnetic transitions).

Doping is another method used to improve the magnetic properties. For example, enhancement of the properties (T_{IM} and T_C) is observed with addition of silver to the $La_{0.7}Ca_{0.3}MnO_3$ target (5 wt%) [102] or with $La_{2/3}Sr_{1/3}MnO_3$ films doped with Ag and grown by dual-beam PLD [103].

2.1.2. Double and triple perovskites: $A_3Mn_2O_7$ and $A_4Mn_3O_{10}$. Although the majority of studies have been done on the simple perovskites $AMnO_3$, colossal magnetoresistance also occurs in $(La, A)_3Mn_2O_7$ (A = Ca, Sr). These compounds are the Ruddlesden–Popper phases whose general formula is $A_{n+1}B_nO_{3n+1}$. Two parents of this family were synthesized in thin-film form with $n = 2$ and $n = 3$.

Films of $La_{2-2x}Ca_{1+2x}Mn_2O_7$ ($x = 0.3$) were deposited on (001)-oriented MgO by single-target magnetron sputtering [104, 105]. *c*-axis-oriented films of $La_{2-2x}Sr_{1+2x}Mn_2O_7$ ($x = 0.4$) can be grown on (001)-oriented $SrTiO_3$ under certain conditions (above 900 °C for the deposition temperature and below 100 mTorr for the oxygen partial pressure; figure 4) [106] which are different from the typical conditions for growing (La, Sr)MnO_3 films. On $SrTiO_3$ substrates, the resistivity curves show a transition at 100 K which coincides with a magnetic transition for $La_{2-2x}Sr_{1+2x}Mn_2O_7$ films on $SrTiO_3$ [106]. Films on MgO are *a*-axis oriented, which means that the long parameter is in the plane of the substrate; these films show evidence of two types of ferromagnetic ordering that possibly result from anisotropic exchange interactions for $0.22 < x < 0.55$ [107]. Magnetoresistance is observed over a wide temperature range below that of the ferromagnetic transitions for MgO and is accompanied by a hysteresis for $SrTiO_3$ [106]. Epitaxial films of (La, Sr)$_3Mn_2O_7$ can also be grown artificially by atomic layer stacking of SrO and (La, Sr)MnO_3 [108].

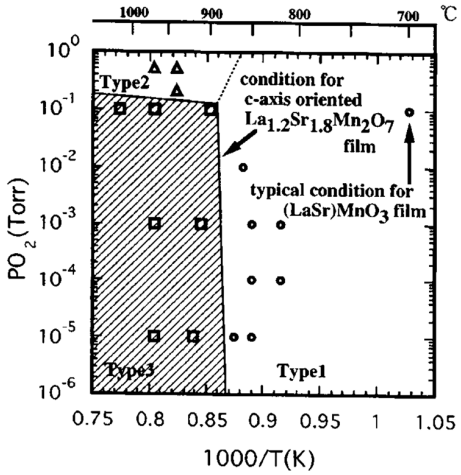

Figure 4. A map of the reaction conditions for different manganite thin films on $SrTiO_3$. The growth conditions for the *c*-axis-oriented (La, Sr)$_3Mn_2O_7$ films (type 3) are restricted to the hatched region. The detailed structures of films of type 1 (open circles) and type 2 (open triangles) are not identified. (Reproduced from reference [106].)

Unlike the previous compound, $La_{3-3x}Ca_{1+3x}Mn_3O_9$ ($x = 0.3$) can be stabilized, but only in the form of thin films and not in the form of bulk [109]. Features similar to those reported for the double perovskite ($n = 2$) were also observed for the $n = 3$ compound, indicating a correlation between the dimensionality (or the *c*-axis bond configuration) and the magnetotransport properties [109].

Thus, it appears that increasing the *c*-axis lattice parameter reduces the magnitude of the CMR at low temperature and this may be attributed to the increased magnitude of the double-exchange transfer matrix and a better ferromagnetic spin alignment.

2.1.3. The particular case of the ordered double perovskite Sr_2FeMoO_6. This review focuses on manganite thin films, but it is also interesting to present the results on the ordered double perovskite Sr_2FeMoO_6, even though it does not contain Mn, since it exhibits magnetoresistance (reference [110]) with a Curie temperature above 370 K. Films of Sr_2FeMoO_{6-y} were grown, using pulsed laser deposition on (001)-oriented $SrTiO_3$ [111, 112]. They are grown on both (001)- and (111)-oriented $SrTiO_3$ but in a narrow window near 900 °C and 10^{-6} Torr [113].

Asano *et al* [111] have shown that by altering the growth conditions they are able to induce either positive (35%) or negative (−3%) magnetoresistance at 5 K under a magnetic field of 8 T. The films show metallic conductivity with a ferromagnetic transition above 400 K [113]. The experimental magnetic moment is calculated to be 4 μ_B per formula unit [112] in agreement with the theoretical one [110]. Sr_2FeMoO_6 films also exhibit both an electron-like ordinary Hall effect and a hole-like anomalous Hall contribution [114]. More importantly, an intergrain tunnelling-type low-field magnetoresistance [115], even at room temperature [113, 116], has been reported.

2.2. Structure and microstructure

It is of prime importance to carry out structural characterization of the films, since it has been shown that in the bulk material, a slight variation of the Mn–O bond length or bond angle drastically modifies the physical properties. Consequently, careful characterization of $AMnO_3$ films is paramount, especially from the crystal structure point of view [117].

One of the best techniques for studying the local structure of thin films, as for bulk, is most probably high-resolution transmission electron microscopy (HREM). Van Tendeloo *et al* [118] have studied the evolution of the microstructure as a function of the thickness in $La_{0.7}Sr_{0.3}MnO_3$ films on $LaAlO_3$. Close to the interface, both the film and the substrate are elastically strained in opposite directions in such a way that the interface is perfectly coherent. In the thicker films, the stress is partly relieved after annealing by the formation of misfit dislocations. Similar results were found for $La_{1-x}Ca_xMnO_3$ [19], where the bottom part of the film, close to the substrate, is perfectly coherent with the substrate, suggesting an important strain, while the upper part shows a domain structure. The perfect epitaxy between the film and the substrate can also be viewed in the cross-section of $Pr_{0.5}Ca_{0.5}MnO_3$ deposited on $SrTiO_3$ (figure 5). This film is grown in the [010] direction, i.e. $2a_P$, perpendicular to the substrate plane. The cross-section along the [110] direction of the substrate clearly shows the perfect coherence of the interface since the [100] or [001] directions of the film match the [110] direction of the substrate. The lattice parameter length in this direction is $a_P\sqrt{2}$.

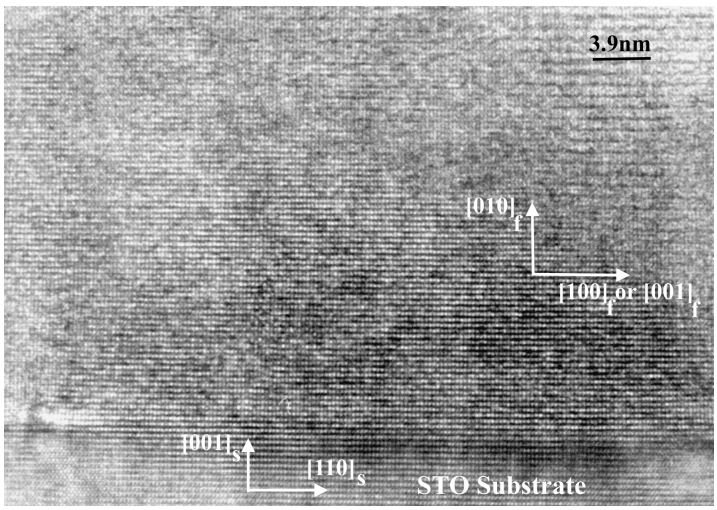

Figure 5. An [010] cross-section of $Pr_{0.5}Ca_{0.5}MnO_3$ deposited on $SrTiO_3$ taken at room temperature.

In general, a strain is observed due to the epitaxial growth in very thin films; i.e. lattice parameters take the values of those of the cubic lattice (see an example of a compressive strain on $SrTiO_3$ [119, 120]). In ultrathin films (60 Å) of $La_{0.73}Ca_{0.27}MnO_3$ on $SrTiO_3$, the crystal structure imposed by the substrate is different to that imposed by the bulk [120] and leads to disorder effects [121] or the formation of different phases such as $(La_{0.7}Sr_{0.3})_3Mn_2O_7$ in $La_{0.7}Sr_{0.3}MnO_3$ films [122]. Microstructural studies also reveal a slight distortion of the $La_{1-x}Ca_xMnO_3$ film, possibly leading to a breakdown of the symmetry from orthorhombic to monoclinic (due to the presence of spots in the electron pattern that are not allowed in the *Pnma* space group) [19]: this suggests that the structural situation might be different in thin film and in bulk material. In contrast, Teodorescu *et al* show that the structure and the stoichiometry of the bulk target are perfectly reproduced in $La_{0.60}Y_{0.07}Ca_{0.33}MnO_{3-\delta}$ thin films [123].

A comparative study of $La_{2/3}Ba_{1/3}MnO_3$ (LBMO) and $La_{2/3}Sr_{1/3}MnO_3$ (LSMO) grown on $SrTiO_3$ shows that thick LBMO presents perfect epitaxy and grows coherently strained throughout the film thickness, whereas the LSMO films are composed of two layers separated by an intrinsic interface region containing a high density of defects [124]. Sometimes, secondary phases are observed [24]. In $Pr_{0.7}Sr_{0.3}MnO_3$ [64], the deposition temperature influences the microstructure and is, thus, directly connected to T_C, which is depressed perhaps due to the role of the grain boundaries.

Returning to the structural characterization of CMR thin films, there are roughly three tendencies that emerge from these studies. The first is that the manganite films are much more sensitive to substrate-induced stress than the analogous cuprate superconductors. The second deals with the presence of two regimes of strain relaxation: one highly strained regime located close to substrate and another above, which is more relaxed. It is not clear exactly where the interface is located or even if it exists in every film. The last interesting feature that has been shown by several groups is the difference in crystal symmetry (lattice parameters, space group, ...) between the thin film and the corresponding bulk material.

2.3. Physical measurements

The standard characterization of CMR thin films consists of resistance measurements versus temperature in zero field and under an applied magnetic field, using the four-probe technique, and also magnetization measurements. Results pertaining to strain effects will be discussed in the next section.

2.3.1. Surface measurements. Several groups focused their studies on the surface [125–127]. Extensive thin-film surface studies were performed using two complementary techniques: atomic force microscopy (AFM) and magnetic force microscopy (MFM) [128–130]. Work was mostly on $La_{1-x}Sr_xMnO_3$ since this material exhibits the highest Curie temperature. It was also found that the properties of the surface are different from those of the bulk from both the electronic and the composition point of view [127]. For example, the surface termination and the Ca surface concentration depend on the overall Ca concentration in $La_{1-x}Ca_xMnO_3$ films [125] (the La/Ca ratio differs between the surface and in the film). The surface of $La_{0.5}Ca_{0.5}MnO_3$ and $La_{0.66}Ca_{0.33}MnO_3$ show a highly ordered grain pattern induced by strains [126], and the $La_{0.65}Sr_{0.35}MnO_3$ surface exhibits a surface phase transition at 240 K (to be compared to 370 K for the bulk) [127].

2.3.2. Transport across a grain boundary (GB). Grain boundaries (GB) strongly affect the properties of CMR materials. Low-field magnetoresistance (LFMR) has been reported and attributed to the spin-dependent scattering of polarized electrons at the GB [131]. Researchers

tried to enhance this property by artificially creating an interface between two elements. We will describe here only the intrinsic effect across natural GB (in polycrystalline thin films) and across artificial GB (in films deposited on bicrystal substrates). The precise influence of the substrate will be discussed separately. Note that another method has been utilized to create artificial GB by scratching the $LaAlO_3$ substrate before the deposition of the LCMO film [132]. The MR is subsequently in a field of 2 kOe and varies with the field orientation with respect to the GB.

The simplest way of creating a natural GB is to grow the film on polycrystalline substrates [133]. Most of this work was done by IBM [133, 134] on La–Ca–Mn–O (LCMO) and La–Sr–Mn–O (LSMO) films. The ρ–T curve of such films depends on the grain size, as shown in figure 6: resistivity in zero field decreases when the grain size increases, but the peak temperature of approximately 230 K is almost independent of the grain size [133]. Gu *et al* show that the low-field magnetoresistance at low temperature has a dramatic dependence on the nature of the in-plane GB [135]. The reduction of zero-field low-temperature resistivity might be explained by the spin-polarized tunnelling across half-metallic grains. Another possibility for obtaining polycrystalline samples is to decrease the deposition temperature. The resulting GB results from a lower crystalline quality of the film [136].

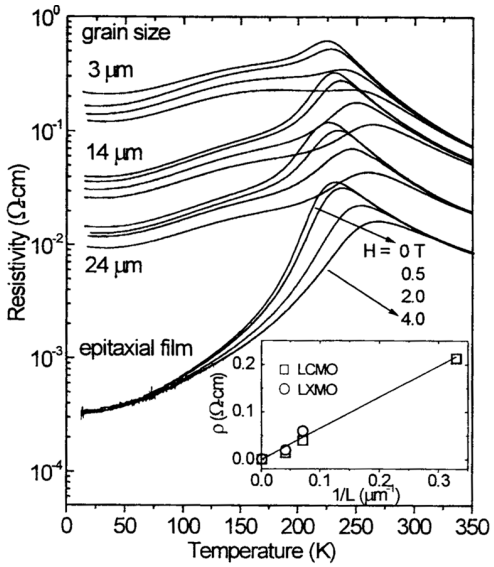

Figure 6. $\rho(T)$ under different magnetic fields for polycrystalline $La_{0.7}Ca_{0.3}MnO_3$ (LCMO) films with different grain sizes and an epitaxial film. The inset shows the zero-field resistivity at 10 K as a function of the average grain size for $La_{0.75}MnO_3$ (LXMO). (Reproduced from reference [133].)

Bicrystal substrates having a single GB have also been used to study the transport across a GB. LCMO and LSMO thin films were deposited on bicrystalline $SrTiO_3$ substrates having a specific misorientation angle [137, 138]. To measure the properties of the GB only, the film was patterned into a Wheatstone bridge. The GB resistance and its magnetic field dependence are strongly dependent on the misorientation angle [138] (see figure 7). The MR increases with increase of the misorientation angle of the bicrystal [138]. The change of resistance is 3% under a 2 mT magnetic field at 300 K for $La_{0.7}Sr_{0.3}MnO_3$. At 77 K, a large bridge resistance (27%) is observed during magnetic field sweeps between $\pm$200 mT over a temperature range down to 77 K. Steenbeck *et al* utilized $La_{0.8}Sr_{0.2}MnO_3$ films grown on $SrTiO_3$ bicrystals with

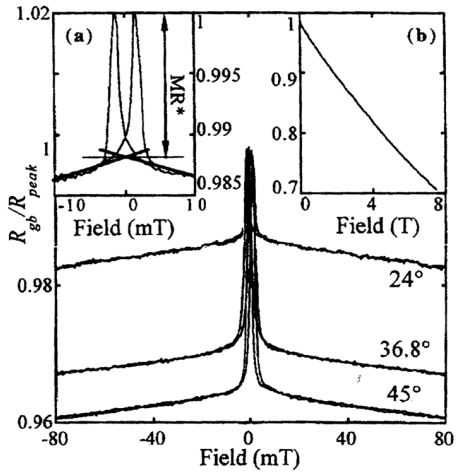

Figure 7. Normalized GB MR as a function of the applied field for different bicrystal angles measured at room temperature. The insets show the (a) low-field and (b) high-field dependences for the 24° device. The applied magnetic field is in the plane and perpendicular to the GB. (Reproduced from reference [138].)

a misorientation angle of 36.8° [139] or 24° [140]. They found that the GB magnetoresistance occurs at low temperature, separated from the intrinsic MR near T_C, and that the sign of the MR at the GB depends on the domain structure and H [139]. Moreover, current–voltage measurements show that the field dependence might not be related to the tunnelling [141].

2.3.3. Irradiation effects. Irradiation, varying the ions dose [142, 143], was used to look at the effect of columnar defects upon the thin-film properties [129, 142]. On irradiated $La_{0.7}Sr_{0.3}MnO_3$ samples, the MFM shows the existence of magnetic domains in different magnetization directions, suggesting that the defects can be considered as pinning centres for the magnetic domain walls [129, 143, 144]. The effect of irradiation (with 90 MeV ^{16}O) on $La_{0.75}Ca_{0.25}MnO_3$ was studied. At a low dose of 10^{11} ions cm^{-2}, the irradiation induces an increase of both the Curie temperature and of the resistive transition temperature T_{IM}, whereas for high doses a decrease is observed [145] due to enhancement of pinning for the magnetic domain walls. The film becomes insulating and does not show any resistivity peak when the dose is higher than 10^{14} ions cm^{-2} (see figure 8) [145]. Irradiation with 250 MeV Ag^{17+} induces phase transformation in $La_{0.7}Ca_{0.3}MnO_3$ thin films [144] indicating that the nature of the ions also plays a role.

2.3.4. Phase separation. Phase separation was suspected in $La_{0.4}Ba_{0.1}Ca_{0.5}MnO_3$ films [146] and it was confirmed by the noise probe method [147] in $La_{2/3}Ca_{1/3}MnO_3$ films; in this work the authors attribute the origin of the random telegraph noise to a dynamic mixed-phase percolative process, where manganese clusters switched back and forth between two phases that differ in their conductivity and magnetization. This spatial inhomogeneity in doped manganite thin films was also investigated in $La_{1-x}Ca_xMnO_3$ [148] using scanning tunnelling microscopy. The phase separation is observed below the Curie temperature where different structures of metallic and more insulating areas coexist and are field dependent. This suggests that the insulator-to-metal transition at T_C should be viewed as a percolation of metallic ferromagnetic domains.

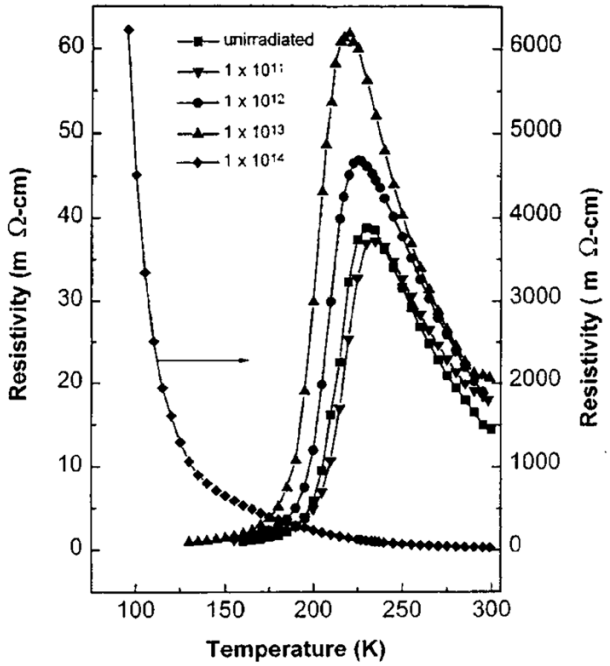

Figure 8. $\rho(T)$ for as-deposited films and irradiated films at different ion doses. (Reproduced from reference [147].)

2.3.5. Other experiments. Magneto-optical measurements reveal the onset of the ferromagnetic transition via the coercive-field increase and the Kerr rotation [149]. Using this technique, the spontaneous formation of twins in $La_{2/3}Ca_{1/3}MnO_3$ films below 105 K was also observed [150].

3. Effects of strains

The CMR manganites are sensitive to all types of perturbation. In particular, it has been shown in bulk that the internal (through the average size of the A-site cation) or external pressure (via hydrostatic pressure) can strongly influence the magnetotransport properties. Since the beginning of the rediscovery of the CMR effect in Mn-based compounds, many studies have been focused on the strains in thin films. This is due to the fact that Mn e_g electrons, which determine most of the physical properties, are coupled to the lattice degrees of freedom through the Jahn–Teller trivalent manganese. Thus, strains affect the properties of the manganite thin films, and, in consequence, one needs to correctly understand the effects in order to obtain the desired properties. The following section will discuss the two types of strain: in-plane (i.e. substrate-induced strains; section 3.1) and out-of-plane strain (i.e. thickness dependence; section 3.2).

3.1. Substrate-induced strains

The first important factor for successful thin-film growth is undoubtedly the substrate. For CMR materials, the same substrates as were used for the HTSC compounds were utilized. The substrates most commonly used to grow manganite perovskites are MgO (cubic, $a = 4.205$ Å),

$SrTiO_3$ (STO, cubic, $a = 3.905$ Å), $LaAlO_3$ (LAO, pseudocubic, $a = 3.788$ Å), $NdGaO_3$ (NGO, orthorhombic, $a = 5.426$ Å, $b = 5.502$ Å and $c = 7.706$ Å) and Si (cubic, $a = 5.43$ Å). Many authors have investigated the strain effects of the substrate by growing various films on different substrates [63, 151–154]. They have experimentally [21, 75, 128, 155–159] or theoretically [160] studied the effect of strains on the magnetoresistive properties of $La_{0.7}Sr_{0.3}MnO_3$ and $La_{0.7}Ca_{0.3}MnO_3$ or on the surface flatness [161] for many substrates. The physical properties of these materials depend on the overlap between the manganese d orbitals and oxygen p orbitals, which are closely related to the Mn–O–Mn bond angle and the Mn–O distance. As the unit cell of the thin film is modified with respect to that of the bulk material, the Mn–O distances and Mn–O–Mn angles are altered, inducing variations in the electronic properties. We will review the main characteristics, such as the structure and the physical properties, which are affected by the substrate-induced strains.

3.1.1. Modification of the structure and the microstructure. The influence of the substrate upon the microstructure/structure, the lattice parameters, the texture and also the orientation of the film is discussed in this section

Using magnetic force microscopy, Kwon *et al* [128] showed on $La_{0.7}Sr_{0.3}MnO_3$ a 'feather-like' pattern, indicating an in-plane magnetization on (100)-oriented $SrTiO_3$, while on (100)-oriented $LaAlO_3$, a 'maze-like' pattern corresponding to a perpendicular magnetization anisotropy is seen. A study of this kind was reproduced and extended recently by Desfeux *et al* using other substrates [162].

The influence of the substrate can principally be deduced from the lattice parameters of the film and the effect of strain on lattice parameters has been studied by many groups. These measurements lead to different spin structures. This is evident for $La_{1-x}Sr_xMnO_3$ for which the spin–orbital phase diagram was obtained in the plane of strain field (c/a ratio) versus doping x using a density-functional electronic calculation [163]. The phase diagram of $La_{0.67}Sr_{0.33}MnO_3$ was also plotted for different substrates [157]. A strong dependence of the anisotropy and Curie temperature on the lattice strain is observed. The effect of uniaxial strain was studied theoretically by Ahn and Millis [164]. Uniaxial strain produces changes in the magnetic ground state, leading to dramatic changes in the band structure and optical spectrum.

Both in-plane and out-of-plane lattice parameters are often modified by stain effects when various substrates are used [68, 75, 157, 165]. This is evidenced in figure 9 for 300 Å thin films of $Pr_{0.7}Sr_{0.3}MnO_3$ (PSMO) grown on $LaAlO_3$, $SrTiO_3$ and $NdGaO_3$ [63]. The 002 peaks of the PSMO/LAO and PSMO/STO films are at 46.2° and 47.8°, corresponding to an out-of-plane parameter of 3.93 and 3.81 Å, respectively (the diffraction peak of the PSMO film on NGO is almost indistinguishable from the substrate peak due to the small mismatch). These values have to be compared to the lattice parameter close to 3.87 Å found in the bulk PSMO. They indicate that the films are under tensile stress on STO (decreasing in the growth direction and expanding in the plane) and under compressive stress on LAO (decreasing in the plane and expanding in the out-of-plane direction) due to the lattice mismatch between the film and the substrate at room temperature (figure 10). The strain effects on the out-of-plane lattice parameter of $La_{0.7}Ca_{0.3}MnO_3$ (LCMO) are enhanced with annealing [166]: the lattice expansion is 2–3 times larger in LCMO/STO than in LCMO/NGO. The stress also influences the bond lengths and bond angles. Miniotas *et al* have evaluated the Mn–O and Mn–Mn distances in $La_{1-x}Ca_xMnO_3$ films grown by MBE. The Mn–O bond length was found to be fixed at 1.975 Å, independent of the substrate type, while the Mn–Mn distance (and subsequently the Mn–O–Mn bond angle) were calculated to be 3.93 Å for STO and 3.84 Å for LAO [167].

Lattice mismatch (i.e. the difference between the parameters of the film and the substrate) influences not only the parameters of the film but also the texture (or epitaxy), i.e. the in-plane

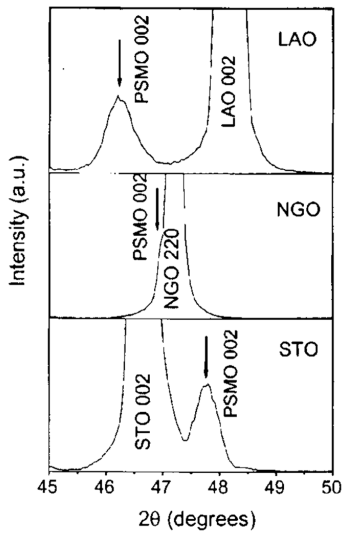

Figure 9. The XRD pattern in the range 45–50° for 300 Å thick $Pr_{0.67}Sr_{0.33}MnO_3$ films on $LaAlO_3$, $NdGaO_3$ and $SrTiO_3$. The arrows indicate the 002 peaks of $Pr_{0.67}Sr_{0.33}MnO_3$. (Reproduced from reference [63].)

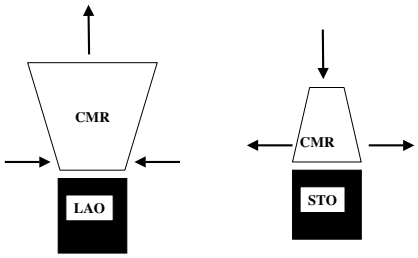

Figure 10. The schematic structure of a film grown under tensile and compressive stress in the plane. Note the compression or the elongation of the out-of-plane parameter, depending on the nature of the stress.

alignments. Usually, changes in the in-plane orientation are observed only when the mismatch is small (e.g. they are seen for LCMO on LAO [168] and not realized on YSZ [169] or on MgO [75]). Textured $La_{2/3}Sr_{1/3}MnO_3$ films were obtained on Si when buffer layers [28, 72] were used. $La_{0.7}Ca_{0.3}MnO_3$ was grown using a buffer layer of CeO_2 [170] and LSMO with a buffer of YSZ [25] or a double layer of $Bi_4Ti_3O_{12}/SiO_2$ [135, 171]. A highly conducting diffusion barrier layer of TiN has also been utilized recently as a buffer layer [172]. This progress is interesting for technological reasons, especially when using Si substrates.

A surprising effect of lattice mismatch is related to the orientation of the films, especially those that crystallize in an orthorhombic perovskite cell. This was first seen for $YMnO_3$ [173] which is [010] oriented on $SrTiO_3$, but [101] oriented on $NdGaO_3$ or $LaAlO_3$. Similar results were obtained with $Pr_{0.5}Ca_{0.5}MnO_3$ [56, 57], $Pr_{0.7}Sr_{0.3}MnO_3$ [64] and $Pr_{0.7}Sr_{0.3-x}Ca_xMnO_3$ [60]. It seems that this orientation can be generalized for all compounds that crystallize in an orthorhombic structure. This dependence on the orientation with respect to the substrate is explained by the lattice mismatch (σ) which should favour one orientation [174]. Indeed, the mismatch between the film and the substrate can be evaluated using the formula

$\sigma = 100(a_S - a_F)/a_S$ (where a_S and a_F respectively refer to the lattice parameters of the substrate and of the film). For $Pr_{0.5}Ca_{0.5}MnO_3$, the smaller mismatch on $LaAlO_3$ is obtained for the [010] axis in the plane ($\sigma_{LAO} = -0.4\%$), i.e. the [101] axis perpendicular to the substrate plane. In contrast, the smaller mismatch on $SrTiO_3$ ($\sigma_{STO} = 2.2\%$) is found for the [101] axis in the plane and thus the [010] axis normal to the surface of the substrate as found experimentally [174].

3.1.2. Influence on the physical properties. Much work has been done on the influence of strain on the transport properties, but we will also describe how the magnetic properties can be changed. Many groups have focused their studies on the modification of the physical properties [175, 176] by the strain effects since the most common properties such as the insulator-to-metal (T_{IM}) transition and the Curie temperatures (T_C) are affected. In figure 11, Koo *et al* show this clear correlation between the substrate and the physical properties for $La_{0.7}Ca_{0.3}MnO_3$ films: the T_{IM} and maximum MR shift to higher temperature on changing a $SrTiO_3$ substrate to a $LaAlO_3$ substrate [159].

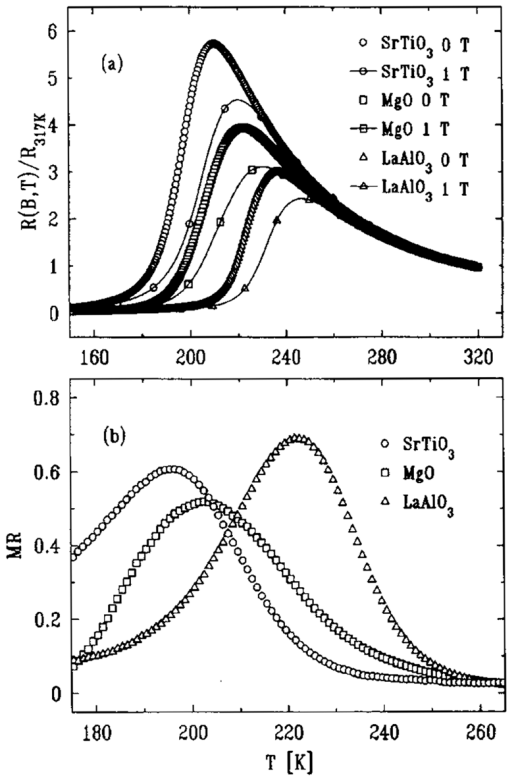

Figure 11. (a) $\rho(T)$ for $La_{0.7}Ca_{0.3}MnO_3$ on various substrates under 0 and 1 T magnetic field. (b) MR defined as $(\rho(0) - \rho(1\text{ T}))/\rho(0))$ normalized to the value at $T = 317$ K. (Reproduced from reference [159].)

Since the crystallinity of these films can be changed, as previously discussed, Gillman *et al* [168] have prepared $La_{1-x}Ca_xMnO_3$ ($x = 0.41$) films on substrates with different lattice parameters by liquid-delivery metal–organic chemical vapour deposition. Films on $LaAlO_3$, closely lattice matched with the substrate, exhibit a high degree of crystallization and a high

magnetoresistance ratio as compared to films deposited on Al_2O_3 or $YZrO_2$. Similar results were reported for $La_{0.8}Sr_{0.2}MnO_3$, which is epitaxial when grown on (100)-oriented $LaAlO_3$ and polycrystalline when grown on (100)-oriented Si [175]. Moreover, T_{IM} increases by 20 K when using (011)-oriented $LaAlO_3$ rather than (001)-oriented $LaAlO_3$. Similar results have been reported for $La_{2/3}MnO_{3-\delta}$ films grown on both Al_2O_3 and $SrTiO_3$ [42] and also for $La_{0.67}Ca_{0.33}MnO_3$ [176]. T_{IM} is higher and the transition is sharper for material grown on STO (300 K) than on ALO (200 K). Even if T_{IM} varies a lot, the Curie temperature is found to remain almost constant, independent of the substrate, for many compounds such as $La_{2/3}MnO_{3-\delta}$ [42] or $La_{0.7}Sr_{0.3}MnO_3$ [177].

The above evidence implies that the T_{IM} is directly related to the substrate type. Often, the transition is at higher temperature and sharper when the mismatch between the film and the substrate is smaller, probably due to a high degree of epitaxy.

Strain influences not only the transport transitions, but also the direction of the magnetization as well (via lattice deformation): it is found to be in-plane for films under tensile stress (for example on $SrTiO_3$) and out-of-plane for compressive stress (as in the case of $LaAlO_3$) [128, 177]. Using a wide-field Kerr microscope, the magnetic domain orientation and contrast of $La_{0.67}Sr_{0.33}MnO_3/SrTiO_3$ suggest a magnetic anisotropy with $\langle 110 \rangle$ easy axes [178]. The easy direction is along [110] for the pseudocubic unit cell, i.e. diagonal to the O–Mn–O bond direction for $La_{0.7}Ca_{0.3}MnO_3$ film grown on untwinned paramagnetic $NdGaO_3(001)$ [179].

The substrate-induced strain can also influence the optical properties, as it does for $La_{0.67}Ca_{0.33}MnO_3$ [180, 181]. This can be explained by the fact that the substrate-induced strain results in modification in the Mn–O bonds and Mn–O–Mn bond angles and, thus, in both the corresponding phonon modes and electron–phonon interactions leading to changes in the phonon frequencies and optical conductance. Note that the strains can also induce a surface magnetization, as for $La_{0.7}Sr_{0.3}MnO_3$ [182].

3.1.3. Low-field magnetoresistance (LFMR). The strain effects on the low-field magnetoresistance (LFMR) were first studied for polycrystalline $La_{0.67}Sr_{0.33}MnO_3$ [133, 134]. They were also extensively studied by Wang *et al* for $Pr_{0.67}Sr_{0.33}MnO_3$ [183–185]. Films with compressive strains (on $LaAlO_3$) show a large LFMR [184] when the field is applied perpendicularly to the substrate plane (figure 12), while they exhibit a positive MR when the film is under tensile stress (on $SrTiO_3$) [183]. Almost no LFMR is observed when the film is stress free (on $NdGaO_3$). O'Donnel *et al* confirmed that the LFMR depends on the strains and the orientation of the field, by studying highly crystallized $La_{0.7}Ca_{0.3}MnO_3$ thin films made by molecular beam epitaxy [81, 90, 186–188]. It was also shown that the LFMR is dominated by the grain boundaries [133, 134] and its sign can be explained by a simple atomic d-state model [89]. This idea of anisotropic MR [165, 189, 190] was evidenced by $La_{0.7}Sr_{0.3}MnO_3$ deposited on (001)-oriented $SrTiO_3$, (110)-oriented $SrTiO_3$ [191] and (110)-oriented $LaGaO_3$. Magnetic anisotropy was also seen recently on $La_{0.7}Ca_{0.3}MnO_3$ films grown on (001)-oriented $NdGaO_3$ [179].

3.1.4. Charge-ordered (CO) manganites. Most of the experimental studies were done on manganites showing an insulator-to-metal transition without field, but it was also shown that substrate-induced strain can affect the properties of charge-ordered (CO) compounds. CO is a phenomenon observed wherein electrons become localized due to the ordering of heterovalent cations in two different sublattices (Mn^{3+} and Mn^{4+}). The material becomes insulating below the CO transition temperature, but it is possible to destroy this state and render the material

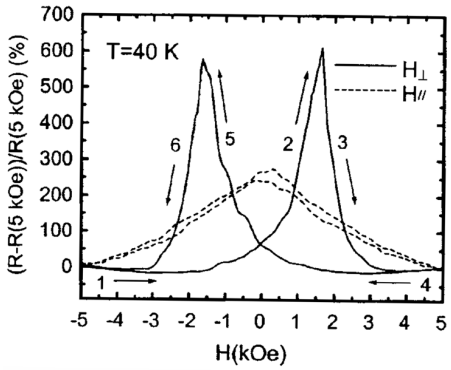

Figure 12. Normalized $R(H)$ curves of 75 Å thick $Pr_{0.7}Sr_{0.3}MnO_3$ films on $LaAlO_3$ measured with the field applied parallel ($H_\parallel$) and perpendicular ($H_\perp$) to the plane of the substrate. In the $H_\perp$-geometry, a very sharp hysteresis loop and large MR ratio are observed. Arrows indicate the scanning sequence of the magnetic field. (Reproduced from reference [183].)

metallic by, for example, the application of a magnetic field [192], but an electric field can also induce insulator–metal transitions in thin films of CO manganites [51]. $Pr_{0.5}Ca_{0.5}MnO_3$ is an example of such a compound. In this case, a tensile stress can decrease the melting magnetic field [56] whereas a compressive strain induces a locking of the structure [57] at low temperature (i.e. under cooling, when the in-plane parameters of the film are equal to the parameters of the substrate, they are kept at this value). This idea of locking was confirmed for $Pr_{0.5}Sr_{0.5}MnO_3$ where the structural and physical transitions are suppressed under cooling [193], as compared to the bulk (note that, while the compound $Pr_{0.5}Sr_{0.5}MnO_3$ is not a typical CO, it has some similarities in physical properties). In this material, the A-type antiferromagnetic phase with the *Fmmm* structure, which is obtained at low temperature (below 135 K) in the corresponding bulk compound, is not observed in the thin film. The consequence of the absence of structural transitions is that magnetotransport properties are affected. There is no antiferromagnetism (i.e. A-type phase) at low temperature. The material only becomes ferromagnetic insulating. This is one of the very few examples of substrate-induced strain upon the film structure. These results show that the strain effect can destabilize the charge-ordered state for CO materials but, surprisingly, it seems also possible to induce a CO state when the film composition is not of CO type (i.e. if the film has an insulator-to-metal transition without the presence of a magnetic field). This has been shown in a normally metallic $La_{0.7}Ca_{0.3}MnO_3$ compound where the lattice-mismatch strain effects lead to a strain-induced insulating state [194]. This insulating behaviour is related to the coexistence of a metallic state with a possibly charge-ordered insulating state [194, 195].

3.2. Thickness dependence

3.2.1. Lattice parameters. The influence of the thickness (t) is primarily seen in the lattice parameters of the films (in-plane and out-of-plane parameters). Usually, the volume of the unit cell is conserved in the thin film as compared to the bulk. In order to verify this result, the evolutions of the three-dimensional strain states and crystallographic domain structures were studied on epitaxial $La_{0.8}Ca_{0.2}MnO_3$ as a function of lattice mismatch with two types of (001) substrate, $SrTiO_3$ and $LaAlO_3$ [196, 197]. Surprisingly, it was shown, using normal and grazing-incidence x-ray diffraction techniques, that the unit-cell volume is not conserved and varies with the substrate as well as the film thickness (figure 13).

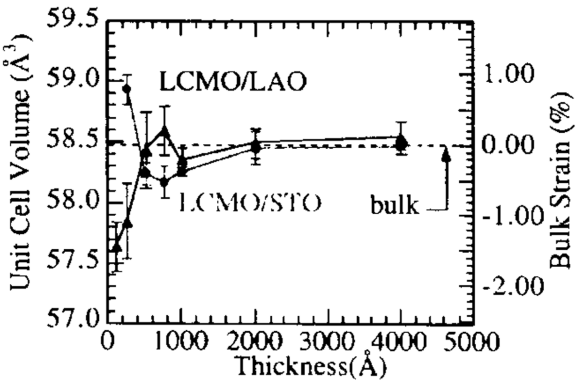

Figure 13. Thickness dependence of the perovskite unit-cell volume of epitaxial $La_{0.8}Ca_{0.2}MnO_3$ films on (001)-oriented $LaAlO_3$ (triangles) and (001)-oriented $SrTiO_3$ (circles). Large deviations of the lattice parameters from those of the bulk are observed. As film thickness increases, both in-plane and out-of-plane lattice parameters tend to deviate away from those of the substrates towards the bulk value. (Reproduced from reference [196].)

But the main result is that for a tensiled film (under expansion in the plane of the substrate), the out-of-plane and in-plane parameters gradually increase and decrease, respectively, as a function of the film thickness [174]. For example, in the case of $Nd_{2/3}Sr_{1/3}MnO_3$ grown on $SrTiO_3$, the out-of-plane parameter increases from a value of 3.8 Å for a 200 Å thick film to 3.86 Å for a 1000 Å film, which is close to the bulk value (figure 14) [198]. The scenario is the opposite when the film is compressively strained as in $La_{0.7}Sr_{0.3}MnO_3$ on (100)-oriented $LaAlO_3$ [199]: the out-of-plane parameter decreases from 3.94 Å for a 300 Å thick film to 3.9 Å for a 4500 Å thick film, while at the same time the in-plane parameter changes from 3.82 Å to 3.88 Å. The film is not completely relaxed until it reaches a thickness of the order of 1000 Å. In $Nd_{0.5}Sr_{0.5}MnO_3$ deposited on (001)-oriented $LaAlO_3$ [50], two regimes were observed using XRD: one which was strained (close to the substrate) and a quasi-relaxed component in the upper part of the film, the latter increasing with film thickness.

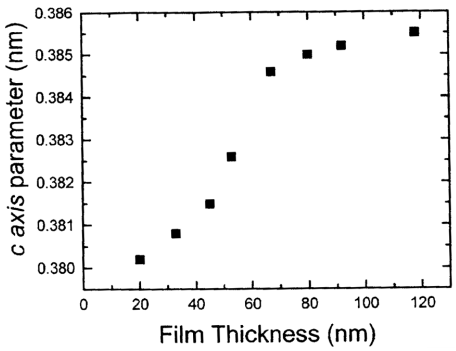

Figure 14. *c*-axis lattice parameter of $Nd_{0.7}Sr_{0.3}MnO_3$ thin films deposited on $SrTiO_3$ as a function of the thickness. (Reproduced from reference [198].)

As previously reported, increasing film thickness leads to a change of the symmetry of the film. This was systematically studied by looking at various film compositions versus thickness by Gorbenko *et al* [154]. They found a strong tetragonal lattice strain using HREM

and XRD characterization. This is more important for a composition in which the bulk structure is orthorhombic, as in $(La_{1-x}Pr_x)_{0.7}Ca_{0.3}MnO_3$, as compared to $La_{1-x}Na_xMnO_3$ or $La_{0.7}Sr_{0.3}MnO_3$ where the structure is rhombohedral [154].

3.2.2. Physical properties. The physical properties of manganites [161, 166, 200] such as insulator-to-metal transition [201, 202], magnetoresistance [155], coercive field [203] and microstructure [121,204,205] are strongly dependent on the thickness. As an example, the MR value (calculated as $\Delta R/R(H)$ for $H = 6$ T) exhibits a strong dependence on film thickness as shown in figure 15 for $La_{0.7}Ca_{0.3}MnO_3$. The curves show a maximum MR for a thickness near 1100 Å with a value of 10^6% and, on either side of the peak, the MR ratio is drastically lower. Transport properties are affected mostly and the magnetization is only moderately changed [200] with thickness, as seen for $La_{0.6}Sr_{0.4}MnO_3$ deposited on MgO or $SrTiO_3$. At an intermediate thickness around 1000 Å, the films usually recover the properties of the bulk compounds. Even when the film is under low epitaxial stress (the case for NGO), T_{IM} varies greatly from 182 K (35 Å) to 264 K (1650 Å), as seen in figure 16 for $La_{0.7}Ca_{0.3}MnO_3$ [201].

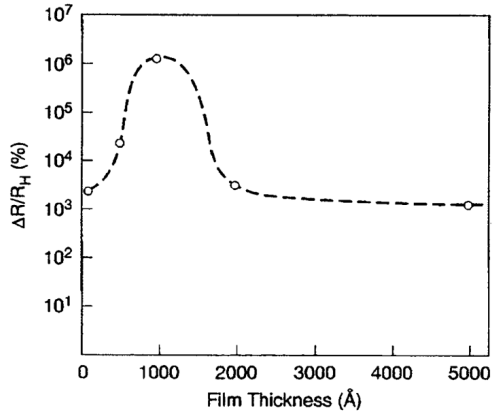

Figure 15. The thickness dependence of the MR for $La_{0.67}Ca_{0.33}MnO_3$ thin films grown on (100)-oriented $LaAlO_3$. (Reproduced from reference [155].)

Films thinner than 1000 Å have properties different from those of the bulk and are most of the time unusual. For example, thin $La_{1-x}Ba_xMnO_3$ film ($t < 1000$ Å) exhibits a value of T_C higher than that of the bulk due to an anomalous tensile strain effect when deposited on $SrTiO_3$. Consequently, the resulting film shows room temperature ferromagnetism and an enhancement of the magnetoresistance [35]. (La, Ca)MnO_3 films, the thinnest films which present full magnetization, grow with the *b*-axis of the structure perpendicular to the substrate, whereas the thicker films grow with the *b*-axis in the plane of the substrate and do not present full magnetization [121]. Another example of the thickness dependence is seen in $La_{0.67}Ca_{0.33}MnO_3$ on $SrTiO_3$, which is ferromagnetic around 150 K but remains insulating [120]. Biswas *et al* [195] have explained this behaviour by the coexistence of two different phases, a metallic ferromagnet (in the highly strained region) and an insulating antiferromagnet (in the low-strain one). This nonuniformity induces, under a magnetic field, an insulator-to-metal transition resulting in a large CMR effect. But the metallic behaviour of bulk $La_{0.7}Ca_{0.3}MnO_3$ can be retained down to a thickness of 60 Å when the $SrTiO_3$ substrate is treated to obtain an atomically flat TiO_2-terminated surface [206]. For $La_{0.9}Sr_{0.1}MnO_3$ ($t < 50$ nm) on (100)-oriented $SrTiO_3$, Razavi *et al* [119] reported an unexpected insulator-

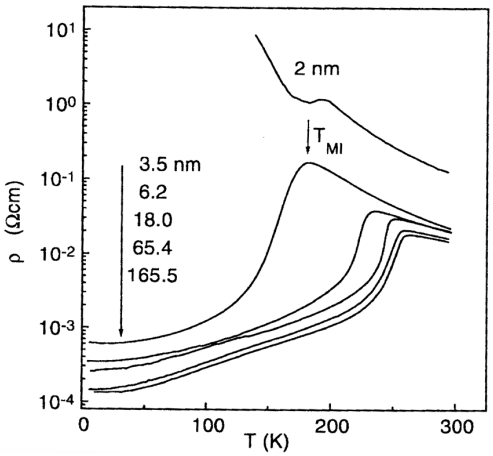

Figure 16. $\rho(T)$ for $La_{0.7}Ca_{0.3}MnO_3$ grown on (110)-oriented $NdGaO_3$ versus film thickness. (Reproduced from reference [201].)

to-metal transition, most probably due to La deficiency. Nevertheless, Sun *et al* [166] have estimated the 'dead layer' for $La_{0.67}Sr_{0.33}MnO_3$ to be around 30 Å for $NdGaO_3$ and 50 Å for $LaAlO_3$ (figure 17). The magnetic, transport and structural properties of $La_{0.7}Sr_{0.3}MnO_3$ deposited on MgO were interpreted recently in terms of a magnetic (10 Å) and an electrical (insulating) dead layer (respectively 10 Å and 4 Å thick) [207].

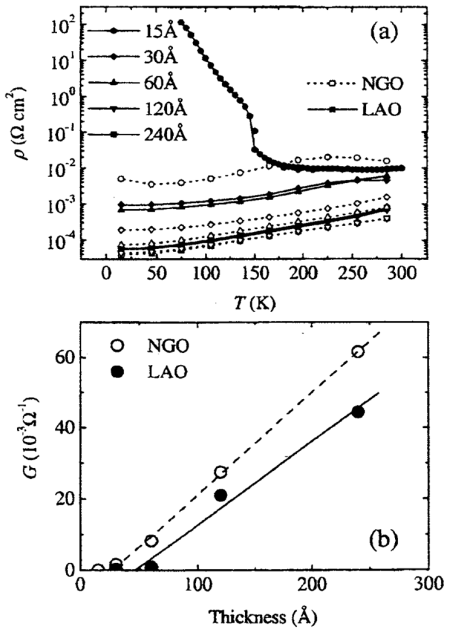

Figure 17. (a) The temperature dependence of the resistivity for $La_{0.67}Sr_{0.33}MnO_3$ films with varying thickness on $NdGaO_3$ and $LaAlO_3$. (b) The thickness dependence of the conductance of films at 14 K. (Reproduced from reference [166].)

More recently, the robustness of the charge-ordered (CO) state was studied by Prellier *et al* [174]. In $Pr_{0.5}Ca_{0.5}MnO_3$, the thicker film induced the less stable state; i.e. a small magnetic field as compared to the case for the bulk is required to destroy the CO state and induce a metallic behaviour (figure 18). In $Nd_{0.5}Sr_{0.5}MnO_3$, the (110) films show a strained and a quasi-relaxed layer. The latter increases with film thickness whereas the strained one has a constant thickness [50]. The coexistence of two strain regimes inside the same film was also seen in $La_{0.66}Ca_{0.33}MnO_3$ films on $SrTiO_3$ [19] and $LaMnO_3$ deposited on $NdGaO_3$ [208]: at the interface a cubic-like dense layer (50 Å thick) is observed while the upper layer shows a

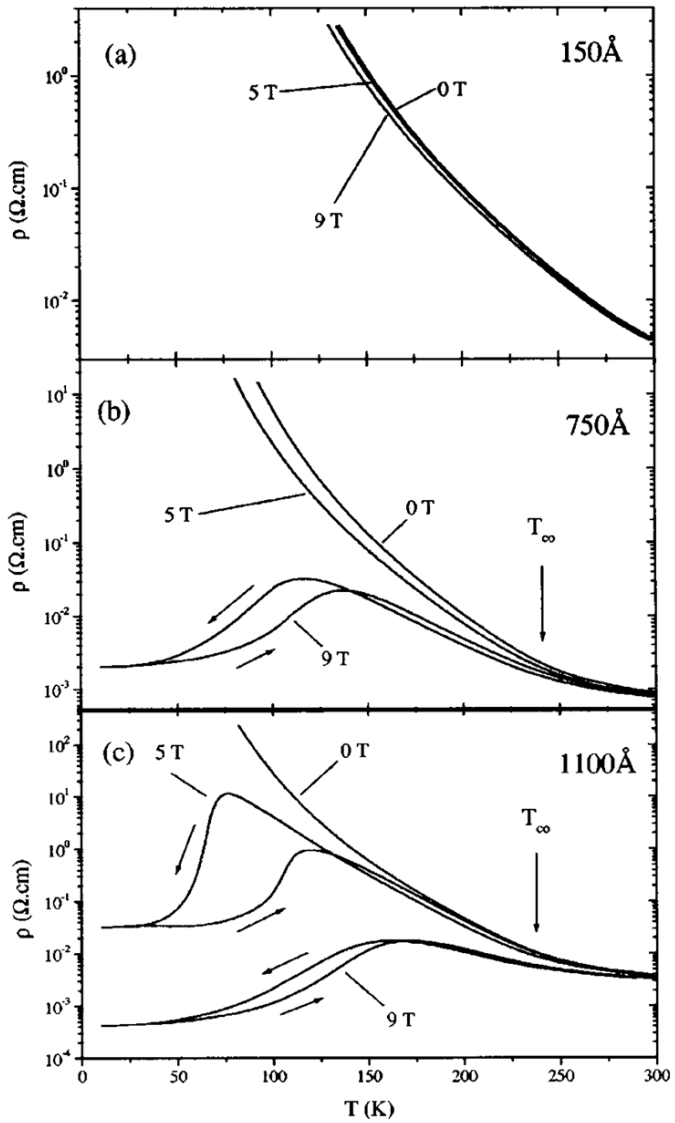

Figure 18. $\rho(T)$ under varying magnetic fields for different thicknesses of $Pr_{0.5}Ca_{0.5}MnO_3$ thin films grown on $SrTiO_3$. Arrows indicate the direction of the temperature dependence. (Reproduced from reference [174].)

columnar growth. These two distinct thickness ranges behave differently with respect to the thickness dependence of the magnetotransport properties [63]; the upper range ($t > 200$ Å) is weakly thickness dependent whereas the lower one is not. These results [63,163] show evidence for the effect of Jahn–Teller-type distortion and confirm theoretical explanations [160]. In $Nd_{2/3}Sr_{1/3}MnO_3$ films, the release of the strain as the thickness increases [198] results in a first-order phase transition.

Thus, these results show the thickness dependence of the physical properties of the film, but it seems difficult to estimate these changes precisely. For example, considering a $Pr_{0.7}Sr_{0.3}MnO_3$ film deposited on $NdGaO_3$, is it possible to evaluate T_{IM} and T_C for 2000 Å thick film? There is no report of such calculations, and one of the reasons is that the properties of the film depend not only of the substrate, but also on the growth conditions. It will be necessary to answer this question in the future.

4. Potential of thin-film growth: the design

The improvement in controlled heterostructures and multilayers is a necessary stage for the realization of many devices and circuits. Structures with new properties such as superlattices were also widely studied.

4.1. New structures

Thin-film methods offer a powerful and versatile technique for growing new structures, as previously seen for example in cuprates. This is due to strain effects that can stabilize structures which do not exist under classical conditions of pressure and temperature. For example, various metastable perovskites, which cannot be formed in bulk or can only be prepared under high pressure, such as $BiMnO_3$ [68], $YMnO_3$ [173] and atomically ordered $LaFe_{0.5}Mn_{0.5}O_3$ [209], are synthesized via a pulsed laser method or by using injection MOCVD, as for $NdMn_7O_{12}$ [210].

Also interesting is the construction of new compounds, such as artificial superlattices, that show unique physical properties since different types of magnetism can be combined by building the desirable structure at the atomic layer level [211]. Growth conditions such as the oxygen pressure or the deposition temperature are easy to control in the thin-film process, allowing the synthesis of metastable phases.

Another approach for obtaining exotic properties via new phases is the method of artificial superlattices. Preliminary films were grown by stacking a magnetic layer ($La_{0.7}A_{0.3}MnO_3$ with A = Sr, Ba, ...) and another perovskite, usually an insulator (such as $SrTiO_3$) [212]. This allows a continuous variation of the in-plane coherency strain in the films [213–215]. High-quality films showing a clear chemical modulation by the presence of satellite peaks around the main diffraction peak were obtained [213,216]. In the case of $La_{0.7}Ca_{0.3}MnO_3$ (LCMO), the metallic transition is suppressed and the MR enhanced at low temperature when the thickness of the LCMO layer is decreased to 25 Å [214]. The MR ($MR = 100[R(0) - R(H)]/R(0)$) is calculated to be 85% at $H = 5$ T over a wide temperature range (10–150 K) (figure 19). A systematic study of $La_{0.7}Ba_{0.3}MnO_3/SrTiO_3$ superlattices shows that the decrease of the $La_{0.7}Ba_{0.3}MnO_3$ (LBMO) layer thickness results in the broadening of the MR peak versus temperature [212]. Such studies also confirm the importance of strains and the relevance of Jahn–Teller electron–phonon coupling in doped manganites, as pointed out by Lu *et al* [213]. Pursuing the same idea, $La_{2/3}Ba_{1/3}MnO_3/LaNiO_3$ multilayers were synthesized. Magnetization measurements show evidence of antiferromagnetic coupling between LBMO layers when the thickness of the $LaNiO_3$ spacer is 15 Å or less [217].

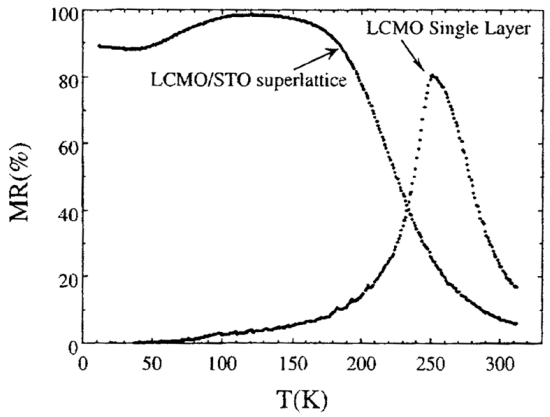

Figure 19. MR (MR = $100[R(0\ \mathrm{T}) - R(5\ \mathrm{T})]/R(0\ \mathrm{T})$) versus temperature for a LCMO (55 Å)/STO (160 Å) superlattice (20 periods) and a single LCMO layer. Note the broadening of the MR peak and the MR of 85% at 5 T from 10 K to 150 K. (Reproduced from reference [212].)

The magnetic exchange interactions in La(Sr)MnO_3/$LaMO_3$ (M = Fe, Cr, Co, Ni) have been extensively studied [218, 219]. It has been shown that the ferromagnetism is systematically affected by the adjacent magnetic layers via the interface, and an expression for T_C was proposed on the basis of the molecular-field image. The magneto-transport properties of superlattices such as $La_{0.6}Pb_{0.4}MnO_3$/$La_{0.85}MnO_3$ [220] or $La_{0.7}MnO_3$/$Pb_{0.65}Ba_{0.05}Ca_{0.3}MnO_3$ [221] were also investigated. An enhancement of the magneto-resistance is obtained in these materials. *c*-axis $YBa_2Cu_3O_7$/$La_{0.67}Ba_{0.33}MnO_3$ superlattices were also grown [222]. Above T_C, the CMR persists up to room temperature, and below T_C the superlattices exhibit a quasi-two-dimensional superconductivity of the $YBa_2Cu_3O_7$ layers coexisting with magnetism in $La_{0.67}Ba_{0.33}MnO_3$ [222]. An increase in the thickness of the antiferromagnetic $La_{0.6}Sr_{0.4}FeO_3$ layer in between $La_{0.6}Sr_{0.4}MnO_3$ layers induces a strong magnetic frustration around the superlattice interfaces, leading to a reduction of the magnetic temperature transition and of the ferromagnetic volume [215].

Salvador *et al* used the PLD technique to create A-site ordering in films of ($LaMnO_3$)/($SrMnO_3$) superlattices [223]. An increase of the superlattice period leads to a decrease in T_C and in T_{IM} or in a low magnetization value.

4.2. Some devices

The intense efforts of the condensed matter community in the area of CMR thin films have led to a more precise understanding of the growth of thin-film oxides, even if the utilization of the materials in devices has not proven viable yet. The aim of this article is to give an overview of the manganite thin films and, for this reason, we will not go into details of the realization of devices. A more comprehensive description of the devices made using CMR materials can be found elsewhere [13]. Examples of devices include magnetic field sensors, electric field devices [224], uncooled infrared bolometers [225] and low-temperature hybrid HTSC–CMR devices [226]. Some of these are briefly discussed below.

A magnetic tunnel junction is a structure composed of two ferromagnetic (FM) layers separated by an insulating barrier (I) and these have attracted attention due to their properties of tunnelling magnetoresistance (TMR). However, to obtain TMR (FM/I/FM junction) with 100% efficiency, it is necessary to have a perfect half-metal (i.e. a 100% spin polarization).

This property was confirmed by spin-resolved photoemission measurements in the case of the $La_{0.7}Sr_{0.3}MnO_3$ (LSMO) compound [227]. Junctions with LSMO which show a TMR effect [228–233]. A large MR of 83% at a low field of 10 Oe at 4.2 K LSMO/STO/LSMO was observed in a trilayer film of [234] (figure 20). Note that the top layer can also be Co [233], half-filled ferrimagnetic Fe_3O_4 [231, 232] or $La_{0.7}Sr_{0.3}MnO_3$ [228, 229]. Using Fe_3O_4, a positive MR is observed which could be attributed to the inverse correlation between the orientations of the carrier spins in the two FM layers [231].

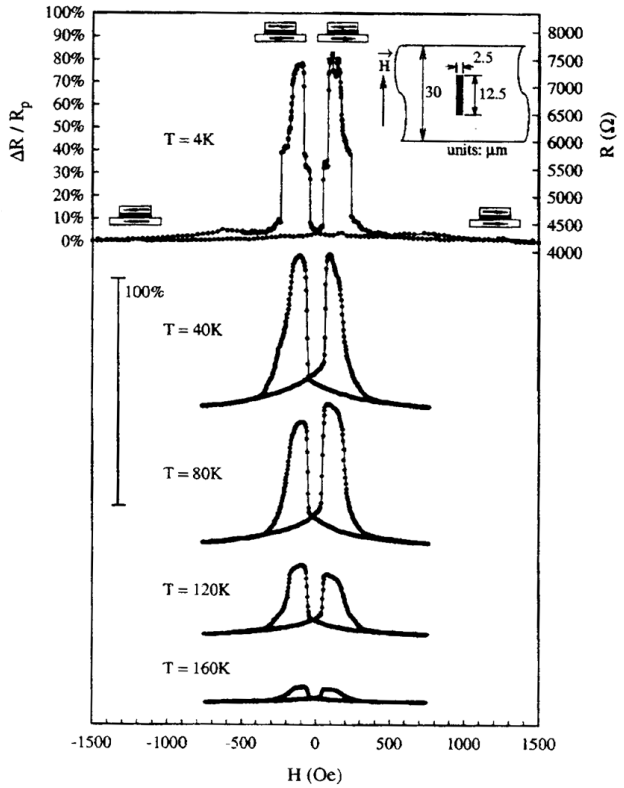

Figure 20. MR versus applied magnetic field at different temperatures for a tunnel junction with a rectangular 2.5 × 12.5 μm top electrode. The moments of both electrodes are shown at various fields. Magnetic field is applied along the easy axis of the rectangle (see the inset). (Reproduced from reference [234].)

The electric field effect has been investigated; here the top layer can be paramagnetic, such as STO [235], or a ferroelectric layer, such as PZT ($PbZr_{0.2}Ti_{0.8}O_3$ [224]), and the bottom layer is a CMR material, but the changes are more profound in the case of PZT where only 3% change in the channel resistance is measured over a period of 45 min at room temperature which makes this material attractive for nonvolatile ferroelectric field-effect device applications [224].

The large temperature coefficient of resistance (TCR, calculated as $(1/R)(\mathrm{d}R/\mathrm{d}T)$) just below the resistivity peak makes these CMR materials interesting for use in bolometric detectors [236, 237]. However, for a given material the TCR decreases as T_C or T_{IM} increase [225]. A TCR of 7% K^{-1} is obtained for LCMO at 250 K.

Hybrid HTSC–CMR structures have also been made for use in spin-injection devices [238–240].

5. Conclusions

The structural, magnetic and transport properties of manganite thin films have been presented in this article. As seen, the colossal-magnetoresistive oxides display an exciting diversity of behaviour in the form of thin films, and an extremely large amount of work has been carried out on thin films showing the great potential of their magnetic and transport properties. It has been shown that the structural and physical properties of these oxides are strongly dependent on the deposition procedure, chemical composition and applied strain. For this reason, the direct comparison between data for a thin film and for a bulk material (ceramic or single crystal) is difficult due to the stress in the thin film.

It has also been shown that devices are of interest and potentially useful as magnetic sensors. Prior to the fabrication of such devices, it will be necessary to characterize the materials more comprehensively, in particular from the viewpoint of the structure and the microstructure. This is clearly evidenced by the fact that intrinsic phenomena such as the substrate-induced strain and the thickness dependence, which are directly related to the thin-film process, strongly affect the magnetotransport properties. These results suggest that the local lattice distortions of the Mn–O bonds in the manganite thin films contribute to changes in the physical properties.

There are two main ideas that should be considered in the future on the basis of recent results. It is now recognized that the strains directly affect the lattice parameters. In addition, researchers have noted that there is a clear relation between the oxygen content (or indirectly the Mn^{3+}/Mn^{4+} ratio) and the lattice parameters of the unit cell of the film. Thus, one should ask the following question: what is the relation between the oxygen content and strain? This triangular connection must be investigated precisely and explained in the future. The second main direction is related to the stress, because despite the large amount of work published on manganite thin films, there is still no direct proof of substrate-induced strains: researchers have only found indirect correlations at room temperature. More sophisticated mechanisms going beyond classical concepts (i.e. looking at the evolution of the structure under cooling) and theoretical studies, in particular quantifying the stress for these oxide films, are required to understand the nature of compounds of this class.

Acknowledgments

We would like to acknowledge Dr A Maignan, Dr A Ambrosini, Professor B Raveau (Laboratoire CRISMAT, Université de Caen), Dr L Mechin (Laboratoire GREYC, ISMRA-Université de Caen), Dr A Anane (Unité mixte CNRS/Thales, Orsay), Dr A M Haghiri-Gosnet (IEF, Université d'Orsay), Professor R L Greene (Center for Superconductivity Research, University of Maryland), Professor P A Salvador (Carnegie Mellon, University of Pittsburgh) and Dr R Desfeux (Université d'Artois) for fruitful discussions and careful reading of this article. We also thank M Morin for helping with the preparation of the manuscript.

References

[1] Jin S, Tiefel T H, McCormack M, Fastnacht R A, Ramesh R and Chen L H 1993 *Science* **264** 413
[2] Jin S, McCormack M, Tiefel T H and Ramesh R 1994 *J. Appl. Phys.* **76** 6929
[3] von Helmolt R, Wecker J, Holzapfel B, Schultz L and Samwer K 1993 *Phys. Rev. Lett.* **71** 2331
[4] von Helmolt R, Wecker J, Samwer K, Haupt L and Bärner K 1994 *J. Appl. Phys.* **76** 6925
[5] McCormack M, Jin S, Tiefel T H, Fleming R M, Phillips J M and Ramesh R 1994 *Appl. Phys. Lett.* **64** 3045
[6] Tokura Y (ed) 1999 *Colossal Magnetoresistance Oxides* (London: Gordon and Breach)

[7] Rao C N R and Raveau B (ed) 1998 *Colossal Magnetoresistance, Charge Ordering and Related Properties of Manganese Oxides* (Singapore: World Scientific)
[8] Okimoto Y, Katsufuji T, Ishikawa T, Urushibara A, Arima T and Tokura Y 1995 *Phys. Rev. Lett.* **75** 109
Wang H Y, Cheong S-W, Ong N P and Batlogg B 1996 *Phys. Rev. Lett.* **77** 2041
Zhao G M, Keller H, Prellier W and Kang D J 2001 *Phys. Rev.* B **63** 172411
[9] Millis A J, Shraiman B I and Mueller R 1996 *Phys. Rev. Lett.* **77** 175
Picket W E and Singh D J 1996 *Phys. Rev.* B **53** 1146
[10] Chrisey D B and Hubler G K (ed) 1994 *Pulsed Laser Deposition of Thin Films* (New York: Wiley–Interscience)
[11] Venkatesan T and Sharma R P 1996 *Mater. Sci. Eng.* B **41** 30
[12] Venkatesan T, Sharma R P, Zhao Y G, Chen Z Y, Lee C H, Cao W L, Li J J, Drew H D, Ogale S B, Ramesh R, Rajeswari M, Wu T, Jin I, Choopun S, Johnson M, Chu W K and Baskaran G 1999 *Mater. Sci. Eng.* B **63** 36
[13] Venkatesan T, Rajeswari M, Dong Z, Ogale S B and Ramesh R 1998 *Phil. Trans.* A **356** 1661
[14] Lawler J F and Coey J M D 1995 *J. Magn. Magn. Mater.* **140–144** 2049
[15] Zeng X T, Wong H K, Xu J B and Wilson I H 1995 *Appl. Phys. Lett.* **67** 3272
[16] Gu J Y, Kim K H, Noh T W and Suh K S 1995 *J. Appl. Phys.* **78** 6151
[17] Lawler J F, Coey J M D, Lunney J G and Skumryev V 1996 *J. Phys.: Condens. Matter* **8** 10 737
[18] Gommert E, Cerva H, Rucki A, von Helmolt R, Wecker J, Kuhrt C and Samwer K 1997 *Appl. Phys. Lett.* **81** 5496
[19] Lebedev O I, Van Tendeloo G, Amelinckx S, Leibold R and Habermeier H U 1998 *Phys. Rev.* B **58** 8065
[20] Prellier W, Rajeswari M, Venkatesan T and Greene R L 1999 *Appl. Phys. Lett.* **75** 1446
[21] Thomas K A, Silva P, Cohen L F, Hossain A, Rajeswari M, Venkatesan T, Hiskes R and MacManus-Driscoll J L 1998 *J. Appl. Phys.* **84** 3939
[22] Guo J Q, Takeda H, Kazama N S, Fukamichi K and Tachiki M 1997 *J. Appl. Phys.* **81** 7445
[23] Cao X W, Fang J and Li K B 2000 *Solid State Commun.* **115** 201
[24] Lu C L, Wang Z L, Kwon C and Jia Q X 2000 *J. Appl. Phys.* **88** 4032
[25] Trajanovic Z, Kwon C, Robson M C, Kim K C, Rajeswari M, Ramesh R, Venkatesan T, Lofland S E, Bhagat S M and Fork D 1996 *Appl. Phys. Lett.* **69** 1005
[26] Snyder G J, Hiskes R, DiCarolis S, Beasley M R and Geballe T H 1996 *Phys. Rev.* B **53** 14 434
[27] Izumi M, Konishi Y, Nishihara T, Hayashi S, Shinohara L M, Kawasaki M and Tokura Y 1998 *Appl. Phys. Lett.* **73** 2497
[28] Fontcuberta J, Ribes M, Martinez B, Trtik V, Ferrater C, Sanchez F and Varela M 1999 *Appl. Phys. Lett.* **74** 1743
[29] Li J, Liu J M, Li H P, Fang H C and Ong C K 1999 *J. Magn. Magn. Mater.* **202** 285
[30] Xiong C S, Pi Li, Xiong Y H, Jia Y B, Zhou G E, Jian Z P and Li X G 2000 *Solid State Commun.* **114** 341
[31] Dulli H, Dowben P A, Liou S H and Plummer E W 2000 *Phys. Rev.* B **62** R14 629
[32] Gonzalez O J, Bistué G, Catano E and Garcia F J 2000 *J. Magn. Magn. Mater.* **222** 199
[33] Robson M C, Kwon C, Kim K-C, Sharma R P, Venkatesan T, Lofland S E, Bhagat S M, Ramesh R, Domínguez M and Tyagi S D 1996 *J. Appl. Phys.* **80** 2334
[34] Zhu X D, Si Weidong, Xi X X, Qi Li, Jiang Q D and Medici M G 1999 *Appl. Phys. Lett.* **74** 3540
[35] Kanki T, Tanaka H and Kawai T 2000 *Solid State Commun.* **114** 267
[36] Sundar Manoharan S, Vasanthacharya N Y, Hegde M S, Satyalakshmi K M, Prasad V and Subramanyam S V 1994 *J. Appl. Phys.* **76** 3923
[37] Srinivasan G, Suresh Babu V and Seehra M S 1995 *Appl. Phys. Lett.* **67** 2090
[38] Yamada Y, Kusumori T and Muto H 2000 *Thin Solid Films* **375** 1
[39] Yamada Y, Kusumori T and Muto H 2000 *J. Appl. Phys.* **88** 6678
[40] Borca C N, Ristoiu D, Xu Q L, Liou S H, Adenwalla S and Dowben P A 2000 *J. Appl. Phys.* **87** 6104
[41] Gupta A, McGuire T R, Duncombe P R, Rupp M, Sun J Z, Gallagher W J and Xiao Gang 1995 *Appl. Phys. Lett.* **67** 3494
[42] Chen C C and de Lozanne A 1998 *Appl. Phys. Lett.* **73** 3950
[43] Zhao Y G, Rajeswari M, Srivastava R C, Biswas A, Ogale S B, Kang D J, Prellier W, Chen Z, Greene R L and Venkatesan T 1999 *J. Appl. Phys.* **86** 6327
[44] Xiong G C, Li Q, Ju H L, Mao S N, Senapati L, Xi X X, Greene R L and Venkatesan T 1995 *Appl. Phys. Lett.* **66** 1427
[45] Xiong G C, Li Q, Ju H L, Greene R L and Venkatesan T 1995 *Appl. Phys. Lett.* **66** 1689
[46] Xiong G C, Li Q, Ju H L, Bhagat S M, Lofland S E, Greene R L and Venkatesan T 1995 *Appl. Phys. Lett.* **67** 3031
[47] Xiong S B, Ding W P, Liu Z G, Chen X Y, Guo X L, Yu T, Zhu Y Y and Hu W S 1996 *Appl. Phys. Lett.* **69** 191
[48] Kasai M, Kuwahara H, Moritomo Y, Tomioka Y and Tokura Y 1996 *Japan. J. Appl. Phys.* **35** L489

[49] Wagner P, Gordon I, Vantomme A, Dierickx D, Can Bael M J, Moshchalkov V V and Bruynseraede Y 1998 *Eur. Phys. Lett.* **41** 49
[50] Prellier W, Biswas A, Rajeswari M, Venkatesan T and Greene R L 1999 *Appl. Phys. Lett.* **75** 397
[51] Ponnambalam V, Parashar S, Raju A R and Rao C N R 1999 *Appl. Phys. Lett.* **74** 206
[52] Wang L M, Sung H H, Su B T, Yang H C and Horng H E 2000 *J. Appl. Phys.* **88** 4236
[53] Kasai M, Kuwahara H, Tomioka Y and Tokura Y 1996 *J. Appl. Phys.* **80** 6894
[54] Oshima H, Miyano M, Konishi Y, Kawasaki M and Tokura Y 1999 *Appl. Phys. Lett.* **75** 1473
[55] Singh S K, Palmer S B, Paul D M^{c}K and Lees M R *Appl. Phys. Lett.* **69** 263
[56] Prellier W, Haghiri-Gosnet A M, Mercey B, Lecoeur Ph, Hervieu M, Simon Ch and Raveau B 2000 *Appl. Phys. Lett.* **77** 1023
[57] Haghiri-Gosnet A M, Hervieu M, Simon Ch, Mercey B and Raveau B 2000 *J. Appl. Phys.* **88** 3545
[58] Lee Y P, Prokhorov V G, Rhee J Y, Kim K W, Kaminsky G G and Flis V S 2000 *J. Phys.: Condens. Matter* **12** L133
[59] Saraf L V, Ogale S B, Chen Z, Godfrey R P, Venkatesan T and Ramesh R 2000 *Phys. Rev.* B **62** R11 961
[60] Mercey B, Lecoeur Ph, Hervieu M, Wolfman J, Simon Ch, Murray H and Raveau B 1997 *Chem. Mater.* **9** 1177
[61] Wagner P H, Metlushko V, Trappeniers L, Vantomme A, Vanacken J, Kido G, Moshchalkov V V and Bruynseraede Y 1997 *Phys. Rev.* B **55** 3699
[62] Wagner P H, Mazilu D, Trappeniers L, Moshchalkov V V and Bruynseraede Y 1997 *Phys. Rev.* B **55** R14 721
[63] Wang H S, Wertz E, Hu Y F, Li Q and Schlom D G 2000 *J. Appl. Phys.* **87** 7409
[64] Mercey B, Wolfman J, Prellier W, Simon Ch, Hervieu M and Raveau B 2000 *Chem. Mater.* **12** 2858
[65] Guo X, Chen Z, Dai S, Zhou Y, Li R, Zhang H, Shen B and Cheng H 2000 *J. Appl. Phys.* **88** 4758
[66] Chen C C and de Lozanne A 1997 *Appl. Phys. Lett.* **71** 1424
[67] Zhao Y G, Li Y H, Ogale S B, Rajeswari M, Smolyaninova V, Wu T, Biswas A, Salamanca-Riba L, Greene R L, Ramesh R and Venkatesan T 2000 *Phys. Rev.* B **61** 4141
[68] Ohshima E, Saya Y, Nantoh M and Kawai M 2000 *Solid State Commun.* **116** 73
[69] Pietambaram S, Kumar D, Singh R K, Lee C B and Kaushik V S 1999 *J. Appl. Phys.* **86** 3317
[70] Lourenço A A C S, Araújo J P, Amaral V S, Tavares P B, Sousa J B, Vieira J M, Alves E, da Silva M F and Soares J C 1999 *J. Magn. Magn. Mater.* **196+197** 495
[71] Ziese M, Sena S P and Blythe H J 1999 *J. Magn. Magn. Mater.* **202** 292
[72] Fontcuberta J, Ribes M, Martinez B, Trtik V, Ferrater C, Sanchez F and Varela M 1999 *J. Appl. Phys.* **85** 4800
[73] Klein J, Höfener C, Alff L and Gross R 2000 *J. Magn. Magn. Mater.* **211** 9
[74] Dörr K, De Teresa J M, Müller K H, Eckert D, Walter T, Vlakhov E, Nenkov K and Schultz L 2000 *J. Phys.: Condens. Matter* **12** 7099
[75] Vlakhov E S, Chakalov R A, Chakalova T I, Nenkov K A, Dörr K, Handstein A and Müller K H 1998 *J. Appl. Phys.* **83** 2152
[76] Zeng X T and Wong H K 1995 *Appl. Phys. Lett.* **66** 3371
[77] Li K, Qi Z, Li X, Zhu J and Zhang Y 1997 *Thin Solid Films* **304** 386
[78] Cheng R, Li K, Wang S, Chen Z, Xiong C, Xu X and Zhang Y 1998 *Appl. Phys. Lett.* **72** 2475
[79] Broussard P R, Qadri S B, Browning V M and Cestone V C 1999 *J. Appl. Phys.* **85** 6563
[80] Chahara K I, Ohno T, Kasai M and Kozono Y 1993 *Appl. Phys. Lett.* **63** 1990
[81] O'Donnel J, Onellion M, Rzchowski M S, Eckstein J N and Bozovic I 1996 *Phys. Rev.* B **54** R6841
[82] Gross R, Alff L, Büchner B, Freitag B H, Höfener C, Klein J, Lu Yafeng, Mader W, Philipp J B, Rao M S R, Reutler P, Ritter S, Thienhaus S, Uhlenbruck S and Wiedenhorst B 2000 *J. Magn. Magn. Mater.* **211** 150
[83] Reutler P, Bensaid A, Herbstritt F, Höfener C, Marx A and Gross R 2000 *Phys. Rev.* B **62** 11 619
[84] Pignard S, Vincent H, Sénateur J P, Fröhlich K and Souc J 1998 *Appl. Phys. Lett.* **73** 999
[85] Dubourdieu C, Audier M, Sénateur J P and Pierre J 1999 *J. Appl. Phys.* **86** 6945
[86] Zhu X R, Shen H L, Li T, Li G X, Zou S C, Tsukamoto K, Yanagisawa T, Okutomi M and Obara A 2000 *Thin Solid Films* **375** 228
[87] Parashar S, Ebenso E E, Raju A R and Rao C N R 2000 *Solid State Commun.* **114** 295
[88] Bae S Y and Wang S X 1996 *Appl. Phys. Lett.* **69** 121
[89] Ziese M and Sena S P 1998 *J. Phys.: Condens. Matter* **10** 2727
[90] O'Donnel J, Eckstein J N and Rzchowski M S 2000 *Appl. Phys. Lett.* **76** 218
[91] Steenbeck K and Hiergeist R 1999 *Appl. Phys. Lett.* **75** 1778
[92] Lecoeur P, Gupta A, Duncombe P R, Gong G Q and Xiao G 1996 *J. Appl. Phys.* **80** 513
[93] Rajeswari M, Shreekala R, Goyal A, Lofland S E, Bhagat S M, Ghosh K, Sharma R P, Greene R L, Ramesh R, Venkatesan T and Boettcher T 1998 *Appl. Phys. Lett.* **73** 2672
[94] Liu J M, Huang Q, Li J, Ong C K, Wu Z C, Liu Z G and Du Y W 2000 *Phys. Rev.* B **62** 8976
[95] Wu W, Wong K H, Li X G, Choy C L and Zhang Y H 2000 *J. Appl. Phys.* **87** 3006

[96] Lobad A I, Averitt R D, Kwon C and Taylor A K 2000 *Appl. Phys. Lett.* **77** 4025
[97] Nam B C, Kim W S, Choi H S, Kim J C, Hur N H, Kim I S and Park Y K 2001 *J. Phys. D: Appl. Phys.* **34** 1
[98] Ju H L, Kwon C, Qi Li, Greene R L and Venkatesan T 1994 *Appl. Phys. Lett.* **65** 2108
[99] Pignard S, Vincent H, Sénateur J P, Pierre J and Abrutis A 1997 *J. Appl. Phys.* **82** 4445
[100] Shreekala R, Rajeswari M, Srivastava R C, Ghosh K, Goyal A, Srinivasu V V, Lofland S E, Bhagat S M, Downes M, Sharma R P, Ogale S B, Greene R L, Ramesh R, Venkatesan T, Rao R A and Eom C B 1999 *Appl. Phys. Lett.* **74** 1886
[101] Choi H S, Kim W S, Nam B C and Hur N H 2001 *Appl. Phys. Lett.* **78** 353
[102] Shreekala R, Rajeswari M, Pai S P, Lofland S E, Smolyaninova V, Ghosh K, Ogale S B, Bhagat S M, Downes M J, Greene R L, Ramesh R and Venkatesan T 1999 *Appl. Phys. Lett.* **74** 2857
[103] Li J, Huang Q, Li Z W, You L P, Xu S Y and Ong C K 2001 *J. Phys.: Condens. Matter* **13** 3419
[104] Asano H, Hayakawa J and Matsui M 1997 *Appl. Phys. Lett.* **70** 2303
[105] Asano H, Hayakawa J and Matsui M 1997 *Japan. J. Appl. Phys.* **36** L104
[106] Konishi Y, Kimura T, Izumi M, Kawasaki M and Tokura Y 1998 *Appl. Phys. Lett.* **73** 3004
[107] Asano H, Hayakawa J and Matsui M 1997 *Phys. Rev.* B **56** 5395
[108] Tanaka H and Kawai T 2000 *Appl. Phys. Lett.* **76** 3618
[109] Asano H, Hayakawa J and Matsui M 1997 *Appl. Phys. Lett.* **71** 844
[110] Kobayashi K I, Kimura T, Sawada H, Terakura K and Tokura Y 1998 *Nature* **395** 677
[111] Asano H, Ogale S B, Garison J, Orozco A, Li Y H, Li E, Smolyaninova V, Galley C, Downes M, Rajeswari M, Ramesh R and Venkatesan T 1999 *Appl. Phys. Lett.* **74** 3696
[112] Westerburg W, Reisinger D and Jakob G 2000 *Phys. Rev.* B **62** R767
[113] Manako T, Izumi M, Konishi Y, Kobayashi K I, Kawasaki M and Tokura Y 1999 *Appl. Phys. Lett.* **74** 2215
[114] Westerburg W, Martin F and Jakob G 2000 *J. Appl. Phys.* **87** 5040
[115] Yin H Q, Zhou J S, Zhou J P, Dass R, McDevitt J T and Goodenough J B 1999 *Appl. Phys. Lett.* **75** 2812
[116] Yin H Q, Zhou J S, Zhou J P, Dass R, McDevitt J T and Goodenough J B 2000 *J. Appl. Phys.* **87** 6761
[117] Prellier W and Raveau B 2001 *J. Phys.: Condens. Matter* **13** 2749
[118] Van Tendeloo G, Lebedev O I and Amelinckx S 2000 *J. Magn. Magn. Mater.* **211** 73
[119] Razavi F S, Gross G, Habermeier H U, Lebedev O, Amelinckx S, Van Tendeloo G and Vigliante A 2000 *Appl. Phys. Lett.* **76** 155
[120] Zandbergen H W, Freisem S, Nojima T and Aarts J 1999 *Phys. Rev.* B **60** 10 259
[121] Aarts J, Freisem S, Hendrikx R and Zandbergen H W 1998 *Appl. Phys. Lett.* **72** 2975
[122] Li Y H, Salamanca-Riba L, Zhao Y, Ogale S B, Ramesh R and Venkatesan T 2000 *J. Mater. Res.* **15** 1524
[123] Teodorescu V S, Nistor L C, Valeanu M, Ghica C, Sandu C, Mihailescu I N, Ristoscu C, Deville J P and Werckmann J 2000 *J. Magn. Magn. Mater.* **211** 54
[124] Wiedenhorst B, Höfener C, Lu Y, Klein J, Alff L, Gross R, Freitag B H and Mader W 1999 *Appl. Phys. Lett.* **74** 3636
[125] Choi J, Zhang J, Liou S H, Dowben P A and Plummer E W 1999 *Phys. Rev.* B **59** 13 453
[126] Peng H B, Zhao B R, Xie Z, Lin Y, Zhu B Y, Hao Z, Tao H J, Xu B, Wang C Y, Chen H and Wu F 1999 *Phys. Rev. Lett.* **82** 362
[127] Dulli H, Plummer E W, Dowben P A, Choi J and Liou S H 2000 *Appl. Phys. Lett.* **77** 570
[128] Kwon C, Robson M C, Kim K-C, Gu J Y, Lofland S E, Bhagat S M, Trajanovic Z, Rajeswari M, Venkatesan T, Kratz A R, Gomez R D and Ramesh R 1997 *J. Magn. Magn. Mater.* **172** 229
[129] Desfeux R, Elard F, Da Costa A, Matthieu Ch, Wolfman J, Hamet J F and Simon Ch 1999 *J. Magn. Magn. Mater.* **196+197** 123
[130] Soh Y A, Aeppli G, Mathur N D and Blamire M G 2000 *J. Appl. Phys.* **87** 6743
[131] Gupta A and Sun J Z 1999 *J. Magn. Magn. Mater.* **200** 24
[132] Srinitiwarawong C and Ziese M 1998 *Appl. Phys. Lett.* **73** 1140
[133] Gupta A, Gong G Q, Xiao G, Duncombe P R, Lecoeur P, Trouilloud P, Wang Y Y, Dravid V P and Sun J Z 1996 *Phys. Rev.* B **54** R15 629
[134] Li X W, Gupta A, Xiao G and Gong G Q 1997 *Appl. Phys. Lett.* **71** 1124
[135] Gu J Y, Ogale S B, Rajeswari M, Venkatesan T, Ramesh R, Radmilovic V, Dahmen U, Thomas G and Noh T W 1998 *Appl. Phys. Lett.* **72** 1113
[136] Teo B S, Mathur N D, Isaac S P, Evetts J E and Blamire M 1998 *J. Appl. Phys.* **83** 7157
[137] Mathur N D, Burnel G, Isaac S P, Jackson T J, Teo B S, MacManus-Driscoll J L, Cohen L F, Evetts J E and Blamire M G 1999 *Nature* **387** 266
[138] Isaac S P, Mathur N D, Evetts J E and Blamire M C 1998 *Appl. Phys. Lett.* **72** 2038
[139] Steenbeck K, Eick T, Kirsch K, O'Donnel K and Steinbeiss E 1997 *Appl. Phys. Lett.* **71** 968
[140] Steenbeck K, Eick T, Kirsch K, Schmidt H G and Steinbeiss E 1998 *Appl. Phys. Lett.* **73** 2506

[141] Todd N K, Mathur N D, Isaac S P, Evetts J E and Blamire M G 1999 *J. Appl. Phys.* **85** 7263
[142] Arora S K, Kumar R, Singh R, Kanjilal D, Mehta G K, Bathe R, Patil S I and Ogale S B 1999 *J. Appl. Phys.* **86** 4452
[143] Ogale S B, Ghosh K, Gu J Y, Shreekala R, Shinde S R, Downes M, Rajeswari M, Sharma R P, Greene R L, Venkatesan T, Ramesh R, Bathe R, Patil S I, Ravikumar R, Arora S K and Mehta G K 1998 *J. Appl. Phys.* **84** 6255
[144] Ogale S B, Li Y H, Rajeswari M, Salamanca-Riba L, Ramesh R, Venkatesan T, Millis A J, Kumar R, Mehta G K, Bathe R and Patil S I 2000 *J. Appl. Phys.* **87** 4210
[145] Bathe R, Date S K, Shinde S R, Saraf L V, Ogale S B, Patil S, Kumar R, Arora S K and Mehta G K 1998 *J. Appl. Phys.* **83** 7174
[146] Hong N H, Sakai J and Imai S 2000 *J. Appl. Phys.* **87** 5600
[147] Raquet B, Anane A, Wirth S, Xiong P and von Molnar S 2000 *Phys. Rev. Lett.* **84** 4485
[148] Fäth M, Freisem S, Menovsky A A, Tomioka Y, Aarts J and Mydosh J A 1999 *Science* **285** 1540
[149] Bobo J F, Magnoux D, Porres R, Raquet B, Ousset J C, Fert A R, Roucau Ch, Baulès P, Casanove M J and Snoeck E 2000 *J. Appl. Phys.* **87** 6773
[150] Vlasko-Vlasov V K, Lin Y K, Miller D J, Welp U, Crabtree G W and Nikitenko V I 2000 *Phys. Rev. Lett.* **84** 2239
[151] Ranno L, Llobet A, Hunt M B and Pierre J 1999 *Appl. Surf. Sci.* **138+139** 228
[152] Yeh N C, Vasquez R P, Beam D A, Fu C C, Huynh J and Beach G 1997 *J. Phys.: Condens. Matter* **9** 3713
[153] Trtik V, Sanchez F, Varela M, Bibes M, Martinez B and Fontcuberta J 1999 *J. Magn. Magn. Mater.* **203** 256
[154] Gorbenko O Yu, Graboy I E, Kaul A R and Zandbergen H W 2000 *J. Magn. Magn. Mater.* **211** 97
[155] Jin S, Tiefel T H, McCormack M, O'Bryan H M, Chen L H, Ramesh R and Schuring D 1995 *Appl. Phys. Lett.* **67** 557
[156] Lofland S E, Bhagat S M, Ju H L, Xiong G C, Venkatesan T, Greene R L and Tyagi S 1996 *J. Appl. Phys.* **79** 5166
[157] Tsui F, Smoak M C, Nath T K and Eom C B 2000 *Appl. Phys. Lett.* **76** 2421
[158] Ju H L, Krishnan K M and Lederman D 1998 *J. Appl. Phys.* **83** 7073
[159] Koo T Y, Park S H, Lee K B and Jeong Y H 1997 *Appl. Phys. Lett.* **71** 977
[160] Millis A J, Darling T and Migliori A 1998 *J. Appl. Phys.* **83** 1588
[161] Okawa N, Tanaka H, Akiyama R, Matsumoto T and Kawai T 2000 *Solid State Commun.* **114** 601
[162] Desfeux R, Bailleul S, Da Costa A, Prellier W and Haghiri-Gosnet A M 2001 *Appl. Phys. Lett.* **78** 3681
[163] Konishi Y, Fang Z, Izumi M, Manako T, Kasai M, Kuwahara H, Kawasaki M, Terakura K and Tokura Y 1999 *J. Phys. Soc. Japan* **68** 3790
[164] Ahn K H and Millis A J 2001 *Phys. Rev.* B **64** 115103
[165] Wu Y, Suzuki Y, Rüdiger U, Yu J, Kent A D, Nath T K and Eom C B 1999 *Appl. Phys. Lett.* **75** 2295
[166] Sun J Z, Abraham D W, Rao R A and Eom C B 1999 *Appl. Phys. Lett.* **74** 3017
[167] Miniotas A, Vailionis A, Svedberg E B and Karlsson U O 2001 *J. Appl. Phys.* **89** 2134
[168] Gillman E S, Li M and Dahmen K H 1998 *J. Appl. Phys.* **84** 6217
[169] Shreekala R, Rajeswari M, Ghosh K, Goyal A, Gu J Y, Kwon C, Trajanovic Z, Boettcher T, Greene R L, Ramesh R and Venkatesan T 1997 *Appl. Phys. Lett.* **71** 282
[170] Zhang W, Wang X, Elliott M and Boyd I W 1998 *Phys. Rev.* B **58** 14 143
[171] Gu J Y, Kwon C, Robson M C, Trajanovic Z, Ghosh K, Sharma R P, Shreekala R, Rajeswari M, Venkatesan T, Ramesh R and Noh T W 1997 *Appl. Phys. Lett.* **70** 1763
[172] Kumar D, Chattopadhyay S, Gilmore W M, Lee C B, Sankar J, Kvit A, Sharma A K, Narayan J, Pietambaram S V and Singh R K 2001 *Appl. Phys. Lett.* **78** 1098
[173] Salvador P A, Doan T D, Mercey B and Raveau B 1998 *Chem. Mater.* **10** 2592
[174] Prellier W, Simon Ch, Haghiri-Gosnet A M, Mercey B and Raveau B 2000 *Phys. Rev.* B **62** R16 337
[175] Krishnan K M, Modak A R, Lucas C A, Michel R and Cherry H B 1996 *J. Appl. Phys.* **79** 5169
[176] Martin F, Jakob G, Westerburg W and Adrian H 1999 *J. Magn. Magn. Mater.* **196+197** 509
[177] Haghiri-Gosnet A M, Wolfman J, Mercey B, Simon Ch, Lecoeur P, Korzenski M, Hervieu M, Desfeux R and Baldinozzi G 2000 *J. Appl. Phys.* **88** 4257
[178] Lecoeur P, Trouilloud P L, Xiao G, Gupta A, Gong G Q and Li X W 1997 *J. Appl. Phys.* **82** 3934
[179] Mathur N D, Jo M H, Evetts J E and Blamire M G 2001 *J. Appl. Phys.* **89** 3388
[180] Boris A V, Kovaleva N N, Bazhenov A V, Samoilov A V, Yeh N C and Vasquez R P 1998 *J. Appl. Phys.* **81** 5756
[181] Vengalis B, Maneikis A, Anisimovas F, Butkute R, Dapkus L and Kindurys A 2000 *J. Magn. Magn. Mater.* **211** 35
[182] Lofland S E, Bhagat S M, Rajeswari M, Venkatesan T, Ramesh R, Gomez R D, Kwon C and Kratz A R 1997

IEEE Trans. Magn. **33** 3964
[183] Wang H S, Wertz E, Hu Y F and Li Q 2000 *J. Appl. Phys.* **87** 6749
[184] Wang H S, Li Q, Liu K and Chien C L 1999 *Appl. Phys. Lett.* **74** 2212
[185] Wang H S and Li Q 1998 *Appl. Phys. Lett.* **73** 2360
[186] O'Donnel J, Onellion M, Rzchowski M S, Eckstein J N and Bozovic I 1997 *Phys. Rev.* B **55** 5873
[187] Eckstein J N, Bozovic I, O'Donnel J, Onellion M and Rzchowski M S 1996 *Appl. Phys. Lett.* **69** 1312
[188] O'Donnel J, Rzchowski M S, Eckstein J N and Bozovic I 1998 *Appl. Phys. Lett.* **72** 1775
[189] Suzuki Y, Wang H Y, Cheong S W and van Dover R B 1997 *Appl. Phys. Lett.* **71** 140
[190] Suzuki Y and Hwang H Y 1998 *J. Appl. Phys.* **85** 4797
[191] Berndt L M, Balbarin V and Suzuki Y 2000 *Appl. Phys. Lett.* **77** 2903
[192] For a review see:
Rao C N R, Arulraj A, Cheetham A K and Raveau B 2000 *J. Phys.: Condens. Matter* **12** R83
[193] Mercey B, Hervieu M, Prellier W, Wolfman J, Simon Ch and Raveau B 2001 *Appl. Phys. Lett.* **78** 3857
[194] Biswas A, Rajeswari M, Srivastava R C, Venkatesan T, Greene R L, Lu Q, de Lozanne A L and Millis A J 2001 *Phys. Rev.* B **63** 184424
[195] Biswas A, Rajeswari M, Srivastava R C, Li Y H, Venkatesan T and Greene R L 2000 *Phys. Rev.* B **61** 9665
[196] Rao R A, Lavric D, Nath T K, Eom C B, Wu L and Tsui F 1998 *Appl. Phys. Lett.* **73** 3294
[197] Nath T K, Rao R A, Lavric D, Eom C B, Wu L and Tsui F 1999 *Appl. Phys. Lett.* **74** 1615
[198] Barman A and Koren G 2000 *Appl. Phys. Lett.* **77** 1674
[199] Suzuki Y, Wu Y, Yu J, Rüdiger U, Kent A D, Nath T K and Eom C B 2000 *J. Appl. Phys.* **87** 6746
[200] Sirena M, Steren L and Guimpel J 2000 *Thin Solid Films* **373** 102
[201] Walter T, Dörr K, Müller K H, Eckert D, Nenkov K, Hecker M, Lehmann M and Schultz L 2000 *J. Magn. Magn. Mater.* **222** 175
[202] Steren L B, Sirena M and Guimpel J 2000 *J. Magn. Magn. Mater.* **211** 28
[203] Steren L B, Sirena M and Guimpel J 2000 *J. Appl. Phys.* **87** 6755
[204] Gross G M, Prauss R B, Leibold B and Habermeier H U 1999 *Appl. Surf. Sci.* **138+139** 117
[205] Prauss R B, Leibold B, Gross G M and Hebermeier H U 1999 *Appl. Surf. Sci.* **138+139** 40
[206] Padhan P, Pandey N K, Srivastava S, Rakshit R K, Kurkarni V N and Budhani R C 2000 *Solid State Commun.* **117** 27
[207] Borges R P, Guichard W, Lunney J G, Coey J M D and Ott F 2001 *J. Appl. Phys.* **89** 3868
[208] Mercey B, Salvador P A, Prellier W, Doan T D, Wolfman J, Hamet J F, Hervieu M and Raveau B 1999 *J. Mater. Chem.* **9** 233
[209] Ueda K, Muraoka Y, Tabata H and Kawai T 2001 *Appl. Phys. Lett.* **78** 512
[210] Bosak A A, Gorbenko O Yu, Kaul A R, Graboy I E, Dubourdieu C, Senateur J P and Zandbergen H W 2000 *J. Magn. Magn. Mater.* **211** 61
[211] Tabata H and Kawai T 1997 *IEICE Trans. Electron.* **80** 918
[212] Kwon C, Kim K C, Robson M C, Gu J Y, Rajeswari M, Venkatesan T and Ramesh R 1997 *J. Appl. Phys.* **81** 4950
[213] Lu Y, Klein J, Höfener C, Wiedenhorst B, Philipp J B, Herbstritt F, Marx A, Alff L and Gross R 2000 *Phys. Rev.* B **62** 15806
[214] Jo M H, Mathur N D, Evetts J E, Blamire M G, Bibes M and Fontcuberta J 1999 *Appl. Phys. Lett.* **75** 3689
[215] Izumi M, Manako T, Konishi Y, Kawasaki M and Tokura Y 2000 *Phys. Rev.* B **61** 12 187
[216] Luo Y, Käufler A and Samwer K 2000 *Appl. Phys. Lett.* **77** 1508
[217] Nikolaev K R, Bhattacharya A, Kraus P A, Vas'ko V A, Cooley W K and Goldman A M 1999 *Appl. Phys. Lett.* **75** 118
[218] Tanaka H, Okawa N and Kawai T 1999 *Solid State Commun.* **110** 191
[219] Tanaka H and Kawai T 2000 *J. Appl. Phys.* **88** 1559
[220] Sahana M, Hedge M S, Prasad V and Subramanyam S V 1999 *J. Appl. Phys.* **85** 1058
[221] Pietambaram S, Kumar D, Singh R K and Lee C B 2001 *Appl. Phys. Lett.* **78** 243
[222] Jakob G, Moshchalkov V V and Bruynseraede Y 1995 *Appl. Phys. Lett.* **66** 2564
[223] Salvador P A, Haghiri-Gosnet A M, Mercey B, Hervieu M and Raveau B 1999 *Appl. Phys. Lett.* **75** 2638
[224] Mathews S, Ramesh R, Venkatesan T and Benedetto J 1997 *Science* **276** 238
[225] Goyal A, Rajeswari M, Lofland S E, Bhagat S M, Shreekala R, Boettcher T, Kwon C, Ramesh R and Venkatesan T 1997 *Appl. Phys. Lett.* **71** 2535
[226] Goldman A M, Vas'ko V, Kraus P A, Nikolaev K and Larkin V A 1999 *J. Magn. Magn. Mater.* **200** 69
[227] Park J H, Vescovo E, Kim H J, Kwon C, Ramesh R and Venkatesan T 1998 *Nature* **392** 794
[228] Kwon C, Xia Q X, Fan Y, Hundley M F and Reagor D W 1998 *J. Appl. Phys.* **83** 7052
[229] Sun J Z, Gallagher W J, Duncombe P R, Krusin-Elbaum L, Altman R A, Gupta A, Yu Lu, Gong G Q and

Xiao G 1996 *Appl. Phys. Lett.* **69** 3266
[230] Viret M, Drouet M, Nassar J, Contour J P, Fermon C and Fert A 1997 *Europhys. Lett.* **39** 545
[231] Ghosh K, Ogale S B, Pai S P, Robson M, Li E, Jin I, Dong Z, Greene R L, Ramesh R and Venkatesan T 1998 *Appl. Phys. Lett.* **73** 689
[232] Ogale S B, Ghosh K, Pai S P, Robson M, Li E, Jin I, Greene R L, Ramesh R, Venkatesan T and Johnson M 1998 *Mater. Sci. Eng.* B **56** 134
[233] De Teresa J M, Barthélémy A, Fert A, Contour J P, Lyonnet R, Montaigne F, Seneor P and Vaurès A 1999 *Phys. Rev. Lett.* **82** 4288
[234] Li X W, Lu Y, Gong G Q, Xiao G, Gupta A, Lecoeur P, Sun J, Wang Y Y and Dravid V P 1997 *J. Appl. Phys.* **81** 5509
[235] Ogale S B, Talyansky V, Chen C, Ramesh R, Greene R L and Venkatesan T 1996 *Phys. Rev. Lett.* **77** 1159
[236] Rajeswari M, Chen C, Goyal A, Kwon C, Robson M C, Ramesh R, Venkatesan T and Lakeou S 1996 *Appl. Phys. Lett.* **68** 3555
[237] Lisauskas A, Khartsec S I and Grishin A 2000 *Appl. Phys. Lett.* **77** 756
[238] Vas'ko V A, Larkin V A, Kraus P A, Nikolaev K R, Grupp D E, Nordman C A and Goldman A M 1997 *Phys. Rev. Lett.* **78** 1134
Vas'ko V A, Nikolaev K R, Larkin V A, Kraus P A and Goldman A M 1998 *Appl. Phys. Lett.* **73** 844
[239] Dong Z W, Ramesh R, Venkatesan T, Johnson M, Chen Z, Pai S P, Shreekala R, Sharma R P, Lobb C J and Greene R L 1997 *Appl. Phys. Lett.* **71** 1718
[240] Yeh N-C, Vasquez R P, Fu C C, Samoilov A V, Li Y and Vakili K 1999 *Phys. Rev.* B **60** 10 522